

**Electrochemical Reactor Simulation for Metal Ion
Removal under Mass Transport Controlled
Conditions**

A Thesis

**Submitted to the College of Engineering
of Nahrain University in Partial Fulfillment
of The Requirements for The Degree of
Master of Science**

in

Chemical Engineering

by

Assan Qussai Naji

B. Sc. 2004

Dhu Al-hijja

1428

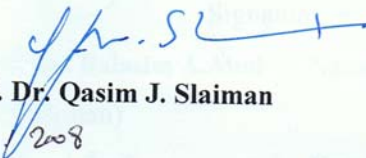
January

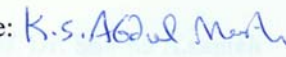
2008

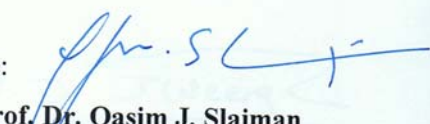
Certificate

Certification

We certify that this thesis entitled "**Electrochemical Reactor Simulation for Metal Ion Removal Under Mass Transport Controlled Conditions**" was prepared by "**Assan Qussai Naji**" under our supervision at Nahrain University / College of Engineering in partial fulfillment of the requirement for the degree of **Master of Science in Chemical Engineering.**

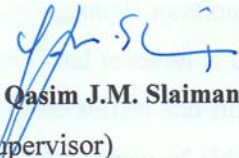
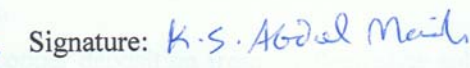
Signature: 
Name: **Prof. Dr. Qasim J. Slaiman**
Date: 21 / 1 / 2008



Signature: 
Name: **Dr. Kamal S. Abdul Masih**
Date: 21 / 1 / 2008

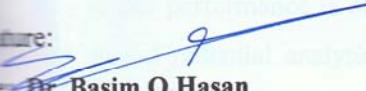
Signature: 
Name: **Prof. Dr. Qasim J. Slaiman**
(Head of Department)
Date: 21 / 1 / 2008

Certificate


We certify, as an examining committee, that we have read this thesis entitled "Electrochemical Reactor Simulation for Metal Ion Removal under Mass Transport Controlled Conditions", examined the student **Basim Qussai Naji** in its content and found it meets the standard of thesis for the degree of Master of Science in Chemical Engineering.

Signature:  Signature: 
Name: **Prof. Dr. Qasim J.M. Slaiman** Name: **Dr. Kamal S. Abdul Masih**
(Supervisor) (Supervisor)
Date: 21/1/2008 Date: 21/1/2008

Signature:  Signature: 
Name: **Ass. Prof. Dr. Balasim A. Abid** Name: **Ass. Prof. Dr. Shatha A. Sameh**
(Chairman) (Member)
Date: 21/1/2008 Date: 21/1/2008

Signature: 
Name: **Dr. Basim O. Hasan**
(Member)
Date: 21/1/2008

Approval of the College of Engineering

Signature: 
Name: **Prof. Dr. Muhsin J. Jweeg**
(Acting Dean)
Date: 24/2/2008

Abstract

In the present work modeling and design of packed bed electrochemical reactor operating under limiting current conditions has been accomplished. The conditions at which simulation model is made are: steady state, one-dimensional, flow-through operation.

The considered reaction is copper deposition from an electrolyte solution containing cupric sulfate and sulfuric acid as a supporting electrolyte with the assumption of the absence of side reactions, the bed is packed with spherical particles.

The effect of three parameters such that: electrolyte flow rate (300, 500, 700, 1000 L / h) and the cross sectional area $= \frac{\pi}{4} D_R^2 = \frac{\pi}{4} 0.04^2 = 1.256637 * 10^{-3} m^2$, feed concentration (0.001 and 0.01 M CuSO₄), and bed thickness 2, 3, and 4 cm on concentration distribution, reaction rate distribution, potential distribution and solution current density distribution have been studied.

The reactor performance is obtained through the solution of equations of mass balance and potential analytically. It is found that: -The electrodeposition rate is increasing when flow rate is increased due to the diffusion boundary layer near the cathode surface become thinner. The electrodeposition rate is increasing when bed thickness is decreased. The electrodeposition rate is increasing when feed concentration is increased, this due to increasing mass transport to the cathode surface.

The potential distribution of the present model is compared with the experimental work of Olive and Lacoste [15] it gave a fairly good agreement.

Variable Notation

<u>Variable</u>	<u>Notation</u>	<u>Unit</u>
γ_a	Activity coefficient of species i	[-]
a	Surface area of bed	[m ⁻¹]
A	Cross sectional area of bed	[m ²]
C _b	Bulk concentration of copper ion	[gmol / Liter]
C _f	Feed concentration of copper ion	[gmol / Liter]
C _s	Surface concentration of copper ion	[gmol / Liter]
D	Diffusion coefficient of copper ion	[m ² / s]
D _R	Bed diameter	[m]
d	Diameter of spherical packing pellet	[m]
E	Cathode potential	[Volts]
E _{eq}	Equilibrium potential	[Volts]
F	Faraday's constant, 96487	[C / eq]
G	Molal free energy	[J / gmol]
k	Mass transfer coefficient	[m / s]
i	Reaction rate	[A / m ²]
i _a	Anodic reaction rate	[A / m ²]
i _c	Cathodic reaction rate	[A / m ²]
i _o	Exchange current density	[A / m ²]
i _L	Local limiting current density	[A / m ²]
I _L	Total applied limiting current density	[A]
L	Bed length	[m]
R	Ideal gas constant=8.314	[KJ/Kg.K]
T	Temperture	[K]

t	Time	[s]
N	no. of moles produced	[mole]
u	Electrolyte velocity based on vacant cross section	[m / s]
x	Instantaneous length	[m]
z	valance	[-]

Greek Letters

<u>Variable</u>	<u>Notation</u>	<u>Unit</u>
α	Transfer coefficient	[-]
ε	Porosity of Bed	[-]
η	Overpotential	[volts]
κ	Electrical conductivity of electrolyte	[ohm ⁻¹ . m ⁻¹]
μ	Electrolyte viscosity	[kg / m.s]
ρ	Electrolyte density	[kg / m ³]
σ	Electrical conductivity of metal	[ohm ⁻¹ . m ⁻¹]
ϕ	Potential	[volts]

List of Contents

Contents	Page
Abstract	i
Variable Notations	iii
List of Contents	iv
List of Tables	vii
List of Figures	x
Chapter One: Introduction	1
1.1 Important Factors in Reactor Performance	1
1.2 Selection of an Electrochemical Reactor	2
1.3 Types of Electrochemical reactor	2
1.4 Examples of Industrial Applications of Flow-Through Porous Electrodes	6
Chapter Two: Literature Survey	8
2.1 Introduction	8
2.2 Basic Components of Electrochemical Reactors	8
2.3 The Nernst Equation	9
2.4 The Rate of an Electrochemical Reaction And Minimum Voltage Requirements for Electrolysis	11
2.5 Reference Electrode	13
2.6 Polarization	16
2.6.1 Activation polarization	18
2.6.2 Concentration Polarization	21
2.7 The Three-Dimensional Porous Electrodes	22
2.7.1 Advantages of Porous Electrode	23
2.8 Heavy Metals Recovery and its Importance	24

2.9	Previous Works	25
2.10	Scope of Present	30
Chapter Three: Mathematical Model and Electrochemical Reactor Design		31
3.1	Introduction	31
3.2	Application of Packed Bed Electrochemical Reactors in Electrodeposition Processes	31
3.2.1	Fixed Bed Electrochemical Reactor	32
3.2.2	3PE Reactor (Pulsed Porous Percolated Reactor)	33
3.2.3	The Porous Cathode of Reticulated Vitreous Carbon (RVC)	33
3.2.4	Kinetic Parameters	34
3.3	Simulation of Electrochemical Processes	37
3.3.1	Porosity Change Inside The Packed Bed	38
3.3.2	Physical Properties	38
3.3.3	Diffusion Coefficient	39
3.4	Mathematical Modeling	39
3.5	Solution of Equations	41
3.6	Electrochemical Reactor Design	44
3.7	Stepwise Procedure For Electrochemical Cell Design	46
3.8	Chapter Four: Results and Interpretations	48
4.1	The Studied Parameters in Present Work	48
4.2	Effect of Flow Rate	49
4.2.1	Concentration Distribution	49
4.2.2	Reaction rate Distribution	51
4.2.3	Potential Distribution	53
4.2.4	Solution Current Density Distribution	55
4.3	Effect of Cupric Sulfate Feed Concentration	57
4.3.1	Concentration Distribution	57
4.3.2	Reaction rate Distribution	60

4.3.3	Potential Distribution	61
4.3.4	Solution Current Density Distribution	62
4.4	Effect of Bed Thickness	63
4.4.1	Concentration Distribution	63
4.4.2	Reaction Rate Distribution	65
4.4.3	Potential Distribution	67
4.4.4	Solution Current Density Distribution	68
	Chapter Five: Discussion	70
5.1	Effect of flow rate	71
5.1.1	Concentration Distribution	71
5.1.2	Reaction Rate Distribution	75
5.1.3	Potential Distribution	78
5.1.4	Solution Current Density Distribution	80
5.2	Effect of Cupric Sulfate Feed Concentration	81
5.2.1	Concentration Distribution	81
5.2.2	Reaction Rate Distribution	82
5.2.3	Potential Distribution	83
5.2.4	Solution Current Density Distribution	84
5.3	Effect of Bed Thickness	86
5.3.1	Concentration Distribution	86
5.3.2	Reaction Rate Distribution	88
5.3.3	Potential Distribution	89
5.3.4	Solution Current Density Distribution	90
5.4	Comparison Between Present Model and Literature	91
	Chapter six: Conclusions and Recommendations	94
6.1	Conclusions	94
6.2	Recommendations	95
	References	

List of Tables

Table	Title	Page
3.1	Stepwise Procedure For Electrochemical Cell Design [40]	46
4.1	Effect of flow rate on the concentration distribution in M for bed thickness of 2 cm, feed concentration 0.001 M	49
4.2	Effect of flow rate on the concentration distribution in M for bed thickness of 3 cm, feed concentration 0.001 M	50
4.3	Effect of flow rate on the concentration distribution in M for bed thickness of 4 cm, feed concentration 0.001 M	50
4.4	Effect of flow rate on the reaction rate distribution (A/m^2) for bed thickness of 2 cm, feed concentration 0.001 M	51
4.5	Effect of flow rate on the reaction rate distribution (A/m^2) for bed thickness of 3 cm, feed concentration 0.001 M	52
4.6	Effect of flow rate on the reaction rate distribution (A/m^2) for bed thickness of 4 cm, feed concentration 0.001 M	52
4.7	Effect of flow rate on the potential distribution (V)for bed thickness of 2 cm, feed concentration 0.001 M	53
4.8	Effect of flow rate on the potential distribution (V)for bed thickness of 3 cm, feed concentration 0.001 M	54
4.9	Effect of flow rate on the potential distribution (V)for bed thickness of 4 cm, feed concentration 0.001 M	54
4.10	Effect of flow rate on the solution current density distribution in (A/m^2) for bed thickness of 2 cm, feed concentration 0.001 M	55
4.11	Effect of flow rate on the solution current density distribution in (A/m^2) for bed thickness of 3 cm, feed concentration 0.001 M	56
4.12	Effect of copperic sulfate concentration on the concentration distribution in (A/m^2) for bed thickness of 2 cm, and flow rates 300 and 500 L / h .	57

4.13	Effect of cupric sulfate concentration on the concentration distribution in (M) for bed thickness of 2 cm, and flow rates 700 and 1000 L / h	58
4.14	Effect of cupric sulfate concentration on the concentration distribution in (M) for bed thickness of 3 cm, and flow rates 300 and 500 L / h	58
4.15	Effect of cupric sulfate concentration on the concentration distribution in (M) for bed thickness of 3 cm, and flow rates 700 and 1000 L / h	59
4.16	Effect of cupric sulfate concentration on the reaction rate distribution in (A/m ²) for bed thickness of 2 cm, and flow rates 300 and 500 L / h	60
4.17	Effect of cupric sulfate concentration on the potential distribution in (A/m ²) for bed thickness of 2 cm, and flow rates 300 and 500 L / h	61
4.18	Effect of cupric sulfate concentration on the solution current density distribution in (A/m ²) for bed thickness of 2 cm, and flow rates 300 and 500 L / h	62
4.19	Effect of Bed thickness on the concentration distribution in (M) flow rate 300 L / h and cupric sulfate concentrations 0.001 and 0.01M	63
4.20	Effect of Bed thickness on the concentration distribution flow rate in(M), 500 L / h and cupric sulfate concentrations 0.001 and 0.01M Table 4.19 and 4.20 show that the when bed theckness increases the downstream concentration will be reduced, i.e. the conversion increases	64
4.21	Effect of Bed thickness on the concentration distribution in (A/m ²), flow rate 300 L / h and cupric sulfate concentrations 0.001 and 0.01M	65
4.22	Effect of Bed thickness on the concentration distribution flow rate in (A/m ²), flow rate 500 L / h and cupric sulfate concentrations 0.001 and 0.01M .	66
4.23	Effect of Bed thickness on the potential distribution in (V), flow rate 300 L / hand cupric sulfate concentrations 0.001 and 0.01M	67
4.24	Effect of Bed thickness on the concentration distribution in (V), flow rate in (V),500 L / h and cupric sulfate concentrations 0.001 and 0.01M	67

4.25	Effect of Bed thickness on the solution current density distribution in (A/m^2) flow rate 500 L / h and copperic sulfate concentrations 0.001 and 0.01M	68
4.26	Effect of Bed thickness on the solution current density distribution in(A/m^2) flow rate 500 L / h and copperic sulfate concentrations 0.001 and 0.01M	69
5.1	Normalized concentration distribution for bed length 2 cm, flow rates 300, 500, 700, and 1000 L / h, and concentrations 0.001 and 0.01 M Cu^{2+} ion Solution	81
5.2	Reaction rate distribution in (A/m^2) for bed length 2 cm, flow rates 300 L / h, and Cu^{2+} ion solution concentrations 0.001 and 0.01 M	82
5.3	Reaction rate distribution in (A/m^2) for bed length 4 cm, flow rates 1000 L / h, and Cu^{2+} ion solution concentrations 0.001 and 0.01 M	82
5.4	Cathode potential distribution (V) for the conditions of $C_f=0.009291M$, $d_p = 0.00208m$, Porosity =0.4 , $E(L) = 0.4V$, and bed length of 1.5 cm given by Olive and Lacoste [15]	92

List of Figures

Figure	Title	Page
1.1	Types of Electrochemical Reactors[3]	5
2.1	A simple electrochemical reactor and its components [9].	9
2.2	The voltage components in a single compartment electrochemical reactor [9].	12
2.3	Measurement of electrode / solution potential differences [9].	14
2.4	Saturated Calomel Electrode system for measurement of electrode potential [9]	15
2.5	Polarization of electrodes: Ideal polarization electrode to the left and to the right ideal nonpolarization electrode [12].	17
2.6	Current density / potential variations for cathodic and anodic polarization of an electrode [13].	20
2.7	Porous electrode configurations [15, 16]	22
3.1	Schematic diagram of the porous electrode reactor to be simulated in present work	32
3.2	Mechanism of mass transport of ions [12]	35
3.3	One-dimensional porous cathode [9].	45
5.1	Concentration distribution in 0.001M Cu ²⁺ ion solution and 2cm bed thickness	71
5.2	Concentration distribution in 0.001M Cu ²⁺ ion solution and 3cm bed thickness	72
5.3	Concentration distribution in 0.001M Cu ²⁺ ion solution and 4cm bed thickness	72
5.4	Concentration distribution in 0.01M Cu ²⁺ ion solution and 2cm bed thickness	73
5.5	Concentration distribution in 0.01M Cu ²⁺ ion solution and 3cm bed thickness	73
5.6	Concentration distribution in 0.01M Cu ²⁺ ion solution and 4cm bed thickness	74
5.7	Reaction rate distribution (A/m ²) in 0.001M Cu ²⁺ ion solution , 2cm bed thickness, and flow rate 300 L / h	75
5.8	Reaction rate distribution (A/m ²) in 0.001M Cu ²⁺ ion solution, 2cm bed thickness, and flow rate 1000 L / h	76

5.9 Reaction rate distribution (A/m^2) in 0.01M Cu^{2+} ion solution, 2cm bed thickness, and flow rate 300 L / h	76
5.10 Reaction rate distribution (A/m^2) in 0.001M Cu^{2+} ion solution, 2cm bed thickness, and flow rate 1000 L / h	77
5.11 Potential distribution (V) in 0.001M Cu^{2+} ion solution, 2cm bed thickness	78
5.12 Potential distribution (V) in 0.001M Cu^{2+} ion solution, 4cm bed thickness	78
5.13 Potential distribution (V) in 0.01M Cu^{2+} ion solution, 2cm bed thickness	79
5.14 Potential distribution (V) in 0.01M Cu^{2+} ion solution, 4cm bed thickness	79
5.15 Solution current density distribution (A/m^2) in 0.001M Cu^{2+} ion solution, 2cm bed thickness	80
5.16 Potential distribution (V) for flow rate 300 L / h, and bed thickness 2 cm	83
5.17 Potential distribution (V) for flow rate 500 L / h, and bed thickness 2 cm	84
5.18 Solution current density distribution in (A/m^2) for flow rate 300 L / h, and bed thickness 2 cm	84
5.19 Solution current density distribution in (A/m^2) for flow rate 500 L / h, and bed thickness 2 cm	85
5.20 Concentration distribution (M) in 0.001M Cu^{2+} ion solution, and flow rate 300 L / h	86
5.21 Concentration distribution (M) in 0.01M Cu^{2+} ion solution, and flow rate 300 L / h	86
5.22 Concentration distribution in 0.001M Cu^{2+} ion solution, and flow rate 500 L / h	87
5.23 Concentration distribution (M) in 0.01M Cu^{2+} ion solution, and flow rate 500 L / h	87
5.24 Reaction rate distribution in (A/m^2) in 0.001M Cu^{2+} ion solution, and flow rate 300 L / h	88
5.25 Reaction rate distribution in (A/m^2) in 0.01M Cu^{2+} ion solution, and flow rate 300 L / h	89

5.26 Potential distribution (V) for flow rate 300 L / h, and feed concentration of 0.001 M	89
5.27 Potential distribution (V) for flow rate 300 L / h, and feed concentration of 0.01 M	90
5.28 Solution current density distribution in (A/m ²) for flow rate 300 L / h, and feed concentration of 0.001 M	90
5.29 Solution current density distribution in (A/m ²) for flow rate 300 L / h, and feed concentration of 0.01 M	91
5.30 Cathode potential distribution for the conditions of $C_f = 0.009291$ M, $d_p = 0.00208$ m, Porosity = 0.4, $E(L) = 0.4$ V, and bed length of 1.5 cm given by Olive and Lacoste [15]	93

Chapter One

Introduction

Electrochemical reactor is defined as any device in which chemical reactions occur directly due to the input of electrical energy. Some of the characteristics of electrochemical processes are reversible in chemical sense, reversible in thermodynamic sense, high material and energy efficiency, high selectivity and product purity, extreme reaction conditions achieved at ambient temperature and pressure, control of structure and surface morphology, low space–time yield, therefore large number of reactor units required, and environmentally benign, low waste [1].

1.1 Important Factors in Reactor Performance

There are many compromises during the process of reactor design/selection in order to accommodate the large number of factors acting as drivers, which are uniform current density distribution, uniform electrode potential distribution, high mass transport rates, ability to handle solid, liquid, or gaseous products, the form of the product and the ease of product extraction, simplicity of design, installation, and maintenance, availability of electrode and membrane materials, capital and running costs, Integration with other process needs [2].

1.2 Selection of an Electrochemical Reactor

It is important to design (or select) an electrochemical reactor for a specific process, so that adequate attention must be paid to the form of the electrode, its geometry and motion, together with the need for cell division or a thin electrolyte gap. The form of the reactants and products and the mode of operation (batch or continuous) are also important design factors.

The desirable factors in reactor design are [2]:

1. Moderate costs (low-cost components, a low cell voltage, and a small pressure drop over the reactor).
2. Convenience and reliability in operation (designed for facile installation, maintenance, and monitoring).
3. Appropriate reaction engineering (uniform and appropriate values of current density, electrode potential, mass transport, and flow).
4. Simplicity and versatility, in an elegant design, which is attractive to the users.

1.3 Types of Electrochemical Reactors

There are several types of electrochemical reactors, which can be classified to [3]: -

1. Tank reactor (Fig. 1.1-a)

This is a simple reactor, which has been used for many years in the metallurgical and chloro-alkali industries.

2. Filter press reactor (Fig. 1.1-b)

This reactor can operate at superatmospheric pressure with electrode gap to about 2 mm. The accumulation of gases between electrodes is a problem in this type, whose severity increase with decreasing electrode gap.

3. Capillary gap reactor (Fig. 1.1-c)

This type was developed primarily for operation with single phase, non-aqueous electrolytes and is used in commercial production of organics. Pumping power is relatively high but a small fraction of total power for the process.

4. Swiss roll reactor (Fig. 1.1-d)

This is a rolled sandwich of flexible sheets or mesh electrodes with thin cloth or net separators in electrode gaps around 1 mm.

5. Fixed bed reactor (Fig. 1.1-e)

Fixed beds or porous matrices can be used as electrode, and it is well suited to processing multiphase electrolyte and give good gas-liquid, liquid-liquid and solid-liquid mass transport. Fixed beds can operate at relatively low superficial velocity to give high conversion per pass and relatively high space-time yield.

6. Fluid bed reactor (Fig. 1.1-f)

In this type the matrix resistivity is increased by fluidizing the particles with flowing electrolyte. The fluid bed gives good mass transport and has been developed to pilot scale for electowinning metals.

7. Slurry reactor (Fig. 1.1-g)

Suspensions of conductive particles have been used as electrodes in various experimental organic electrosyntheses. Electrode materials used are fine powders such as catalyzed carbon black.

8. Gas diffusion reactor (Fig. 1.1-h)

The electrodes consist of microporous plates with graded porosity and/or wettability. Gaseous reactant diffuses from behind the electrode and reaction takes place along three phase boundaries inside the electrode matrix.

9. Stacked porous electrode reactor (Fig. 1.1-i)

In this device microporous electrode layers are bonded to each side of an ion conducting membrane to give a compact divided cell, three dimensional electrode reactor. SPE reactors originated as fuel cells but have since been applied to water electrolysis and chlor-alkali production.

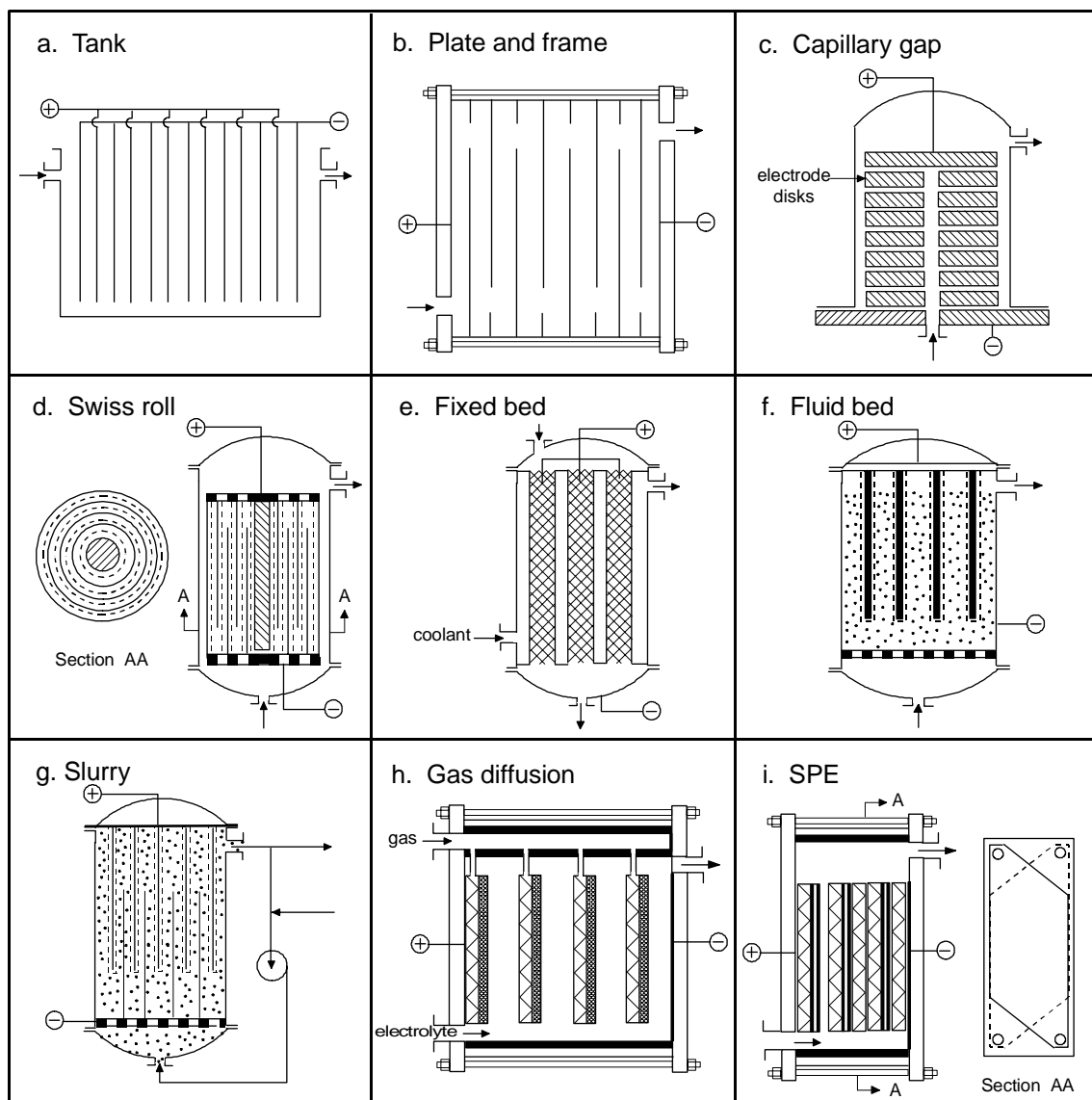


Fig. 1.1 Types of electrochemical reactor [3].

1.4 Examples of Industrial Applications of Electrochemical Reactors

Electro-organic synthesis, which offer opportunities for performing many reactions at controlled rates and at great product selectivity, without added catalysts, than do conventional means [4]. Examples of the electro-organic synthesis are the synthesis of aniline, benzoquinone and p-aminophenol [3]

Electro-organic synthesis techniques can be classified to [5]: -

1. Indirect process: The organic compound being treated does not come into contact with the electrochemical reactor. The process is carried out with previously prepared redox reagent.
2. Direct process: The organic compounds are reacted at the electrode, where they oxidized or reduced and possibly undergo electron transfer induced reactions with themselves or solvent molecules.

Removal of electrodepositive cations by electrodeposition, such as [6]:

Cu from 600 ppm to < 1

Pb from 1.45 ppm to 0.05 ppm from H₂SO₄ solution

Hg from 10 ppm to 0.01 ppm from NaCl solution

Ag processing of waste photographic emulsions

Au from waste plating solution

Oxidation of organic pollutants and CN⁻ (from 24 to 0.1 ppm). Also oxidation of organic surfactant and reducing of foaming in process for manufacturing of Na₂CO₃ [6].

Wastewater treatment: wastewater containing toxic metal ions, such as cadmium, chromium, copper, gold, lead, nickel, silver, tin and zinc, is generated in large quantities during electroplating, manufacturing of microelectronic parts, mining

and processing of photographic films. These toxic metals should be removed from wastewater before discharge for environmental and economic reasons. Although many separation technologies, such as membrane processes and chemical precipitations, are used to remove toxic metal ions, the electrolytic process is attractive because of its ability to remove the contaminants at low operating costs. In addition, the metals in wastewater are recovered for reuse. A variety of electrolytic cells have been designed using porous plate, packed-bed and fluidized –bed electrodes. These have large surface area and high reaction rate per unit volume [7].

The development of design and operation of electrochemical process and devices has remained largely an art before 1981, well past the time when quantitative methods were introduced relevant to the design of ordinary chemical processes. The rather complex interaction between component phenomena in cells, and the hybrid backgrounds in science and engineering necessary for understanding them, are probably responsible for the relative slowness of the development of the electrochemical engineering [1].

Chapter Two

Literature Survey

2.2 Introduction

When a chemical reaction can proceed spontaneously via an ionic mechanism, it is possible in principle to convert part of the energy change directly into electric energy without the intermediaries of a heat engine and generator. Conversely, some chemical reactions can be made to occur, via an ionic mechanism, by the addition of electric energy to a suitable contrived reactor system. Devices for accomplishing either of these ends are called Electrochemical Cells [8].

2.11 Basic Components of Electrochemical Reactors

A simple electrochemical reactor is shown schematically in **Fig. (2.1)**. When an electromotive force (emf) of a sufficient magnitude is applied electron transfer occurs between each electrode and the liquid, resulting in a flow of electricity in the external circuit and chemical reactions at each electrode. This phenomenon is referred to as electrolysis the potential difference between the two electrodes cause a movement of the negatively charged ions, the anions, towards the positive electrode or anode. Simultaneously the positively charged ions known as cations move towards the negative electrode or cathode. The electron flow is in the opposite

direction to the conventional flow of positive electricity but nevertheless it is evident that in a chemical sense oxidation occurs where electrons pass into metallic conductor (at the anode), and reduction where they flow into the ionic media (at the cathode)[1]. The reactor is frequently divided into two compartments by means of an ion exchange membrane made of solid polymer or by a diaphragm which may be made of porous plastic, porous ceramic or asbestos deposits on a gauze. Accordingly the term anolyte is used to denote the electrolyte solution in the anode compartment and catholyte describes the solution in the cathode compartment [6].

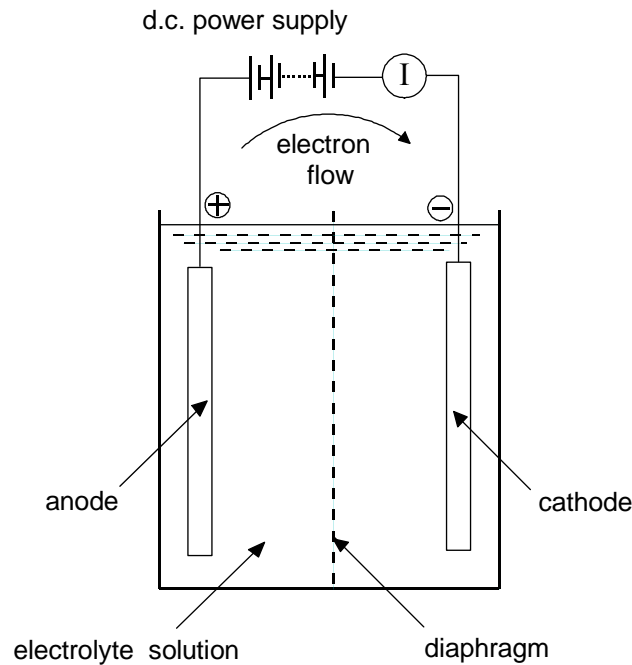


Figure 2.1 A simple electrochemical reactor and its components [9].

2.12 The Nernst Equation

Based on the thermodynamic reasoning, an equation can be derived to express the emf of a cell in terms of the concentrations of reactants and products. The general reaction for a galvanic cell can be assumed to be



The corresponding change of Gibbs free energy of products and reactants, where G_C represents the molal free energy of substance C, etc.

$$\Delta G = (s_D G_D + s_C G_C) - (s_A G_A + s_B G_B) \quad \dots(2.2)$$

A similar expression is obtained for each substance in the standard state or arbitrary reference state, the symbol G° indicating standard molal free energy:

$$\Delta G^\circ = (s_D G_D^\circ + s_C G_C^\circ) - (s_A G_A^\circ + s_B G_B^\circ) \quad \dots(2.3)$$

If a_A is the corrected concentration or pressure of substance A, called its activity, the difference of free energy for A in any given state and in the standard state is related to a_A by the expression

$$s_A (G_A - G_A^\circ) = s_A RT \ln a_A = RT \ln a_A^{s_A} \quad \dots(2.4)$$

where R is the gas constant (8.314 J / gmol.K) and T is the absolute temperature. Subtracting equation (2.3) from (2.2) and equating to corresponding activities, the following expression will be obtained

$$\Delta G - \Delta G^\circ = RT \ln \frac{a_C^{s_C} \cdot a_D^{s_D}}{a_A^{s_A} \cdot a_B^{s_B}} \quad \dots(2.5)$$

When the reaction is at equilibrium, there is no tendency for it to go, $\Delta G = 0$, and

$$K = \frac{a_C^{s_C} \cdot a_D^{s_D}}{a_A^{s_A} \cdot a_B^{s_B}}$$

where K is the equilibrium constant for the reaction. Hence

$$\Delta G^\circ = RT \ln K \quad \dots(2.6)$$

On the other hand, when all the activities of reactants and products are equal to unity, the logarithm term becomes zero ($\ln 1 = 0$) and $\Delta G = \Delta G^\circ$. Since

$\Delta G = -E_{eq} z F$, it follows that $\Delta G^{\circ} = -E_{eq}^{\circ} z F$, where E_{eq}° is the emf when all reactants and products are in their standard state (activities equal to unity). Corresponding to equation (2.5)

$$E_{eq} = E_{eq}^{\circ} - \frac{RT}{zF} \ln \frac{a_C^{S_C} \cdot a_D^{S_D}}{a_A^{S_A} \cdot a_B^{S_B}} \quad \dots(2.7)$$

This is the Nernst equation, which expresses the exact emf of a cell in terms of activities of products and reactants in the cell. The activity a_A of a dissolved substance A is equal to its concentrations in moles per thousand grams of water (molality) multiplied by a correction factor γ , called the activity coefficient. The activity coefficient is a function of temperature and concentration and, except for very dilute solutions, must be determined experimentally.

If reactant A is a gas, its activity is equal to its fugacity, approximated at ordinary pressures by the pressure in atmospheres. The activity of pure solid is arbitrarily set equal to unity, similarly for a substance like water whose concentration is essentially constant throughout the reaction, the activity is set equal to unity [10].

2.13 The Rate of an Electrochemical Reaction And Minimum Voltage Requirements for Electrolysis

Faraday discovered the two laws which express the relationship between amounts of product formed during electrolysis and the quantity of electricity passed. These can be combined in the following statement: the passage of 96487 coulombs through an electrochemical reactor produces in total one gram equivalent of products at an electrode.

$$N_i = \frac{I_i t}{s_i F} \quad \dots(2.8)$$

To estimate the electrolysis voltage requirements for a given process, it is useful to consider the process at equilibrium. For a simple electrochemical process in which only one reaction occurs at each electrode, it is represented by the stoichiometric equation of the reaction **Figure (2.2)** illustrates a simple reactor in which the electrolysis takes place. The reaction represented by equation (2.1) in unnatural process at temperature and pressure of the reactor without applied voltage. This unnatural state is conveniently represented by the positive sign of the free energy change of the reaction, ΔG [9].

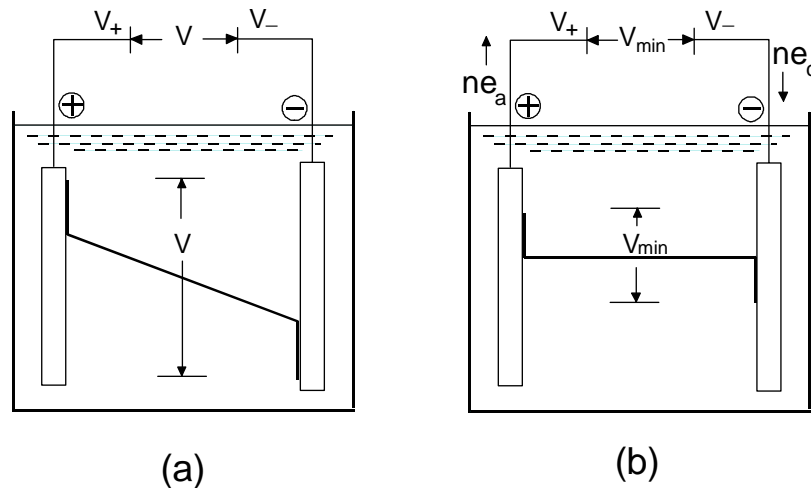


Figure 2.2 The voltage components in a single compartment electrochemical reactor [9]. (a) Finite current (b) Zero current

When the applied voltage (V) is decreased until the current illustrated in Fig.(2.2) is reduced to zero, the solution potential drop necessarily disappears but the two interfacial potential difference remains although they are decreased in magnitude. At this zero current condition the voltage applied keeps the system at an equilibrium state. This voltage is the minimum electrolyzing voltage. At equilibrium the free energy of the system is a minimum and under this condition

$$z\mu_{ec} + s_A\mu_A + s_B\mu_B \rightarrow s_C\mu_C + s_D\mu_D + z\mu_{ea} \quad \dots(2.9)$$

Where μ_A , μ_B , μ_C and μ_D are the chemical potentials of species A, B, C and D respectively, μ_{ec} and μ_{ea} represent an electron consumed and produced at the cathode and anode respectively as indicated in **Figure. (2.1)**. Substitution of equation (2.2) into equation (2.9) and rearranging gives

$$\Delta G = z(\mu_{ec} - \mu_{ea}) \quad \dots(2.10)$$

At equilibrium the chemical potential of an electron in an electrode is equal to the chemical potential of an electron in the adjacent power supply terminals. Thus one can rewrite equation (2.10) as

$$\Delta G = zFV_{min} \quad \dots(2.11)$$

Equation (2.11) enables the minimum electrolyzing voltage for a system to be calculated from free energy data [9].

2.14 Reference Electrode

The *electrical potential* is defined in electrostatics as the work done against the coulombic force in bringing a hypothetical positive charge (a test charge) from infinity to that point. If this charge being brought through a chemical environment, then additional work would have to be done to overcome chemical interaction between the charge and the environment, e.g.

Van Der Waals force. The potential difference between two pieces of copper for example is meaningful on the basis that a test charge would experience chemical interactions of the same type and magnitude in each piece [9].

Strictly speaking one can not talk about a potential difference across an interface because potential difference can only be defined and physically measured between regions nominally of identical chemical composition.

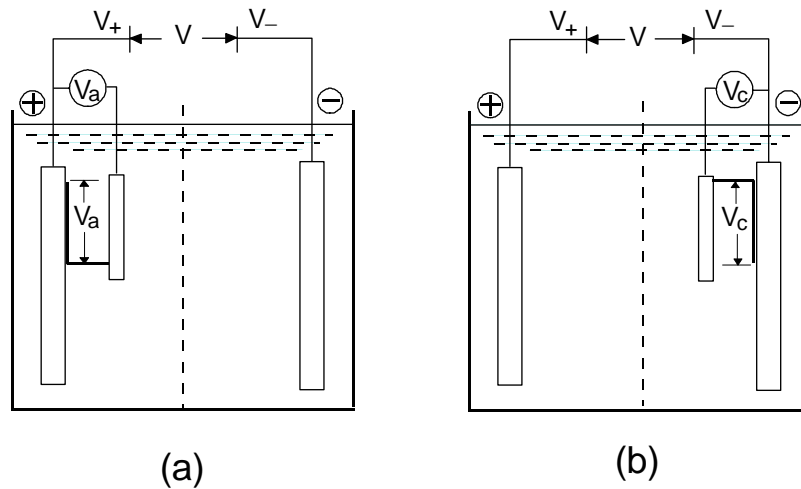


Figure 2.3 Measurement of electrode / solution potential differences [9].
 (a) Anodic (b) Cathodic

To measure the electrode /solution potential difference one need to connect one terminal of a voltmeter to the electrode and other terminal to the solution and this can be done only via another electrode placed in the solution. This second electrode is called a *reference electrode* as shown in Fig.(2.3) [9]. There is no definite rule about the selection of references. A literature search is the best way to find a suitable reference electrode which has been used in the system of interest. If no suitable reference electrode can be found in the literature, the only way to obtain a good reference electrode is by trail and error [11].

A very popular reference electrode is the calomel electrode (Fig.(2.4)) which can be purchased as a compact ready made unit. It consists of metallic mercury covered with a thin layer of calomel (mercurous chloride) in contact with a solution of potassium chloride saturated with mercurous chloride resulting in the following reversible reaction



A saturated solution of potassium chloride is very convenient to use and the potential of a saturated calomel electrode (SCE) is then 0.242V with respect to the standard hydrogen electrode (SHE) at 25 °C with a temperature coefficient of -0.76 mV/°C.

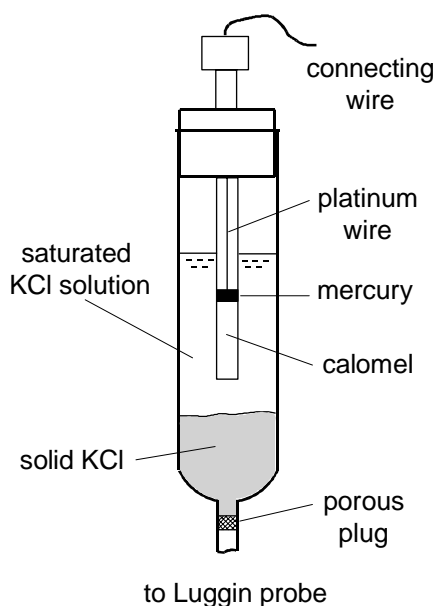


Figure 2.4 Saturated Calomel Electrode system for measurement of electrode potential [9]

2.15 Polarization

Polarization is the departure of the electrode potential (or cell potential) from the reversible (i.e. Nernstian or equilibrium) value upon passage of faradaic current. The larger this departure is the larger the extent of polarization is said to be. The ideal polarized electrode shows a very large change in potential upon the passage of an infinitesimal current; thus ideal polarizability is characterized by a horizontal region of an i - E curve. A substance that tends to cause the potential of an electrode to be nearer its equilibrium value by virtue of its being oxidized or reduced is called a depolarizer. An ideal nonpolarizable electrode (or ideal depolarized electrode) is thus an electrode whose potential does not change due to passage of current, that is, an electrode of fixed potential. Nonpolarizability is characterized by a vertical line on an i - E curve. The extent of polarization is measured by the overpotential, η , which is the deviation of the potential from the equilibrium value [12]. Fig. 2.5 below shows the ideal polarization electrode and the ideal nonpolarization electrode.

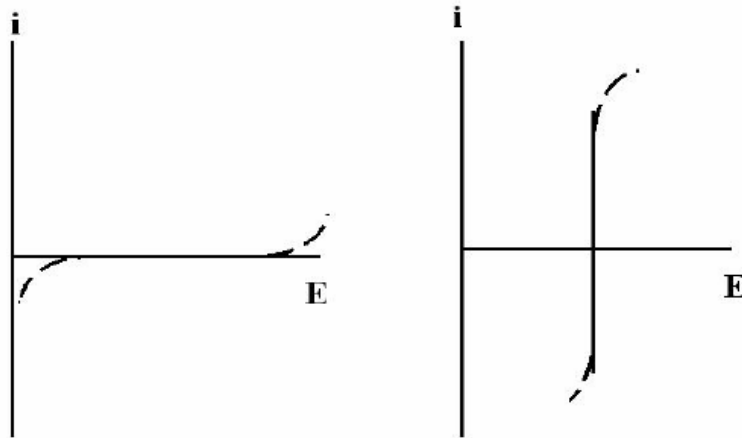


Figure 2.5 Polarization of electrodes: Ideal polarization electrode to the left and to the right ideal nonpolarization electrode [12]

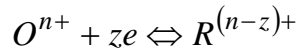
The electrolyzing voltage for a typical electrochemical reactor is expressed as

$$V = V_{min} + \eta_a + |\eta_c| + V_{ohmic} \quad \dots(2.13)$$

where η_a and η_c are the anodic and cathodic overpotentials, and V_{ohmic} represents voltage contribution due to the solution resistance [12].

2.15.1 Activation polarization

The electrode kinetics will be commenced by considering the general electrode reaction. At equilibrium



The letters O and R represent molecules of an oxidized and reduced species respectively.

The equilibrium of the reaction is disturbed by altering the electrode potential.

The current which flows when the electrode is polarized cathodically, represents the difference between the rates of the forward (cathodic) and reverse (anodic) reactions

.The current density (current per unit area), i (reaction rate), which will be considered a positive quantity is in this case given by

$$i = i_c - i_a \quad \dots(2.14)$$

where i_c is the partial current density for the cathodic reaction and i_a that for the anodic reaction. By analogy with chemical kinetics the rate of the forward reaction can be written as

$$\frac{i_c}{zF} = k_c C_{O_s} \quad \dots(2.15.a)$$

$$\frac{i_a}{zF} = k_a C_{R_s} \quad \dots(2.15.b)$$

where k_a and k_c are the electrochemical rate constants and C_{R_s} and C_{O_s} are the concentration of R and O at that point close to the electrode surface respectively

where R is discharged, after substitution

$$i = zFk_c C_{O_s} - zFk_a C_{R_s} \quad \dots(2.16)$$

By using Arrhenius type of rate constant/activation energy relationship, the rate constants k_c and k_a can be expressed in terms of the electrode

potential, which is a measure of the free energy requirements, by the formulas

$$k_c = k_c^o \exp\left[\frac{-\alpha zFE}{RT}\right] \quad \dots(2.17)$$

$$k_a = k_a^o \exp\left[\frac{(1-\alpha)zFE}{RT}\right] \quad \dots(2.18)$$

k_o and $k_o a$ are standard rate constants referenced to some particular electrode potential. Equations (2.17) and (2.18) imply that a fraction, αE , of the cathode potential is effective in promoting the cathodic process, the remainder suppressing the reverse (anodic) process. E is measured relative to the SHE and the quantity α is referred to as the transfer coefficient.

The forms of equations (2.17) and (2.18) are such that a positive increase in i_c and hence i is achieved by making E more negative.

Now elimination of rate constants

$$i = zFk_c^o \exp\left[\frac{-\alpha zFE}{RT}\right] C_{os} - zFk_a^o \exp\left[\frac{(1-\alpha)zFE}{RT}\right] C_{Rs} \quad \dots(2.19)$$

At equilibrium $E = E_{eq}$ the bulk concentrations of O and R denoted by C_{ob} and C_{Rb} respectively are uniform throughout, and $i = 0$ so that

$$i_o = zFk_c^o \exp\left[\frac{-\alpha zFE}{RT}\right] C_{os} - zFk_a^o \exp\left[\frac{(1-\alpha)zFE}{RT}\right] C_{Rs} \quad \dots(2.20)$$

where i_o is called the exchange current density and represents the rates of the forward and reverse reactions at equilibrium. Substitution of equation (2.19) into (2.20) and rearrange gives

$$i = i_o \left\{ \frac{C_{os}}{C_{ob}} \exp\left[\frac{-\alpha zF\eta}{RT}\right] - \frac{C_{Rs}}{C_{Rb}} \exp\left[\frac{(1-\alpha)zF\eta}{RT}\right] \right\} \quad \dots(2.21)$$

Equation (2.21) serves as a general expression for the rate of an electrode reaction in terms of electrode overpotential and known as Butler-Volmer

equation [13]. Fig.2.6 shows the general form of current density-overpotential relationship given by equation (2.19) for both cathodic and anodic overpotential. The lack of symmetry between the anodic and cathodic portions of the curve is quite intentional since a symmetrical plot can only occur if $\alpha = 1/2$ and $C_{Ob} = C_{Rb}$.

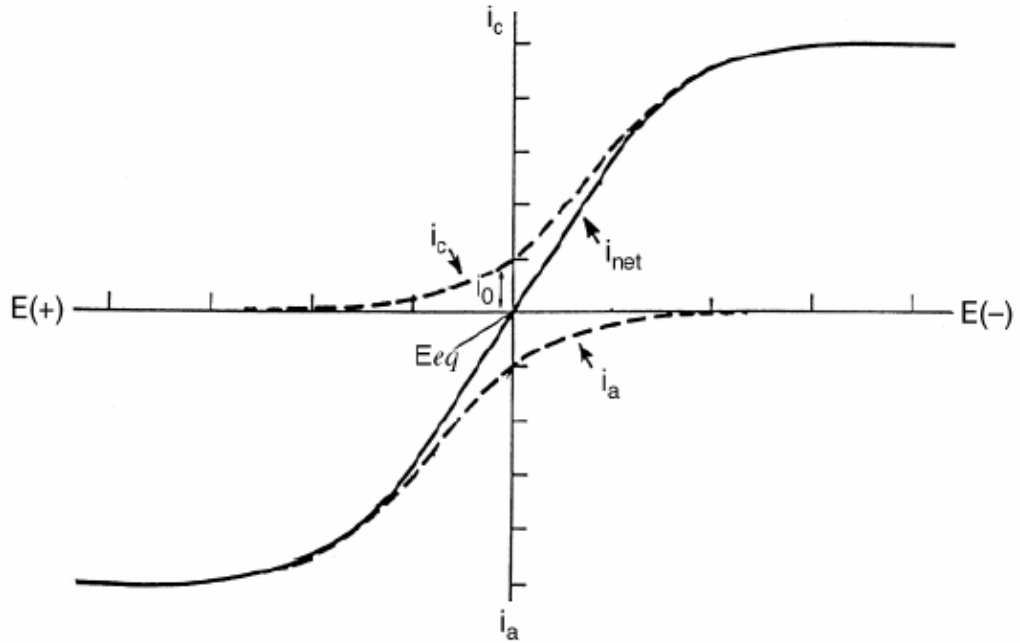


Figure 2.6 Current density / potential variations for cathodic and anodic polarization of an electrode [13].

2.15.2 Concentration Polarization

Is caused by changes in the concentrations of species participating in an electrode reaction. When a current is passing, a depletion or accumulation of some species occurs in the electrolyte solution adjacent to an electrode. The electrode is thus surrounded by a solution of different composition to that in the bulk which would cause a shift in the electrode potential away from its equilibrium value. The overpotential will evidently be reduced if the concentrations of the participating species close to the electrode are maintained as near as possible to their values in the bulk of the solution. This is accomplished by insuring that high rates of mass transfer between the electrode and solution bulk take place by means of stirring or flow of the solution. The larger the current, the smaller is the surface concentration of ions, or the smaller is the C_s ; therefore the larger is the corresponding polarization. Infinite concentration polarization is approached when C_s approaches zero at the electrode surface; the corresponding current density producing this limiting lower value of C_s is called the limiting current density, obviously, in practice, polarization can reach infinity; instead another electrode reaction establishes itself at a more active potential than corresponds to the first reaction [9] (see the mathematical modeling in chapter three).

2.16 Three-Dimensional Porous Electrodes

The application of porous electrodes of high specific surface area and mass transfer coefficient is a promising approach to electrochemical process intensification. At present, porous electrodes are commonly used in chemical power supplies, fuel cells and metal extraction from industrial solutions and wastewater. Fig.2.7a Flow-through electrolyte and current passed in co-currently, Fig.2.7b shows a flow-by two-compartment reactor, and Fig.2.7c shows a flow-through single compartment reactor [15, 16 and 17].

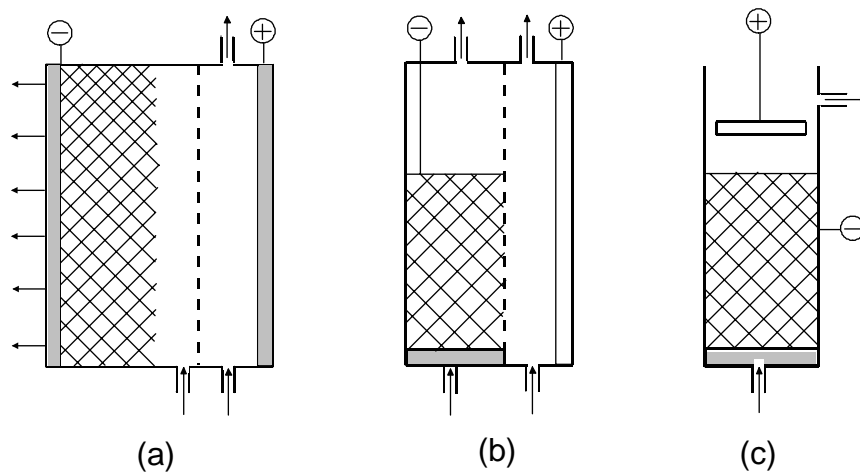


Figure 2.7 Porous electrode configurations [15, 16]

(a) Flow-through electrolyte and current passed in co-currently

(b) Flow-by two compartment reactor

(c) Flow-through electrolyte and current passed in counter-currently.

The main problem in porous electrode theory is the search for conditions providing the most efficient utilization of their extended surface for the performance of the specified main process. These conditions commonly involve attainment of the most uniform potential distribution over the porous electrode depth [18].

2.16.1 Advantages of Porous Electrode

Porous electrodes have numerous industrial applications primarily because they promote intimate contact of the electrode material with the solution. Specific factors are as follows [9, 16]

1. Porous electrode provide a very large electrode area in proportional to their size (e.g. $10^6 \text{ m}^2/\text{m}^3$ volume) and this is several times greater in magnitude than that for non-porous structure and more expensive (typically not greater than $10^2 \text{ m}^2/\text{m}^2$ for a parallel plate system).
2. Double-layer adsorption constitutes the basis for novel separation processes involving cycling of the electrode potential. Just as in conventional fluid-solid adsorption, a high specific interfacial area is desirable.
3. Important reactants may be stored in the solution in close proximity to the electrode surface by means of porous electrodes. This permits sustained high rate discharging of the lead-acid battery.
4. A dilute contaminant can be removed effectively with a flow-through porous electrode. The proximity of the flowing stream to electrode surface is a gain important.

5. Similar arguments apply to non-conducting reactants of low solubility. Then another solid phase (as in batteries) or gas phase (as in fuel cells) may be incorporated into the system, or the reactants may be dissolved and forced through the porous electrode.
6. The compactness of the porous electrode can reduce the ohmic potential drop by reducing the distance through which the current must flow.

2.17 Heavy Metals Recovery and its Importance

Metals contamination in processed water is a serious problem for several industrial sectors such as surface treatment, electroplating and the electronic industry. The outlet wastewater from these industrial processes normally contains a metal concentration higher than the acceptable limit set by law. Therefore, the treatment of contaminated water before it is directly discharged is required in order to reduce the amount of metal to an acceptable level [7]. In its daily operation, the electroplating industry generates a significant amount of discharge water containing heavy metals. Heavy metals are toxic to living organisms and tend to accumulate in the environment over a period of time [20]. The toxicity of heavy metals has been known for many years, and the clinical symptoms of prolonged exposure to a heavy metal contaminated environment are well defined. Heavy metals enter waterways via effluent discharging from electroplating, metal finishing, explosive pigments and paint producing, and metal/mechanics manufacturing industries in general. As a result of high toxicity, the concentration of highly toxic metallic ions in drinking water is restricted to ppb. Besides that the prospect of recovery has attracted interest among industries for environmental and economic reasons. For example, valuable heavy metals are recycled and reused while the outlet water is permitted to discharge to the environment [19].

2.18 Previous Works

This section will be mainly concerned with the previous works for modeling and simulation of porous electrode electrochemical reactor working at both activation control process and mass transfer control process.

The first work on modeling of porous electrode reactor was done by Newman and Tobias (1962)[21], described the behavior of one-dimensional porous electrode from a macroscopic point of view and developed general equations for the prediction of current distribution and reaction rate in such electrode, regardless the geometry of the electrode.

Sioda (1971)[22] derived an equation for the potential distribution in the porous electrode working under limiting current for the condition of a flowing solution. Also he obtained an equation for the ohmic potential drop in the solution between the two ends of the porous electrode.

Alkire and Gracon (1975)[23] investigated experimentally the region of operating conditions where mass transfer restrictions affect behavior and developed a general mathematical model for flow-through porous electrodes for two systems first is the deposition of copper and the second one is the reduction of ferricyanide under limiting current.

Coeuret, Hutin and Gaunad (1976)[24] studied the fixed flow-through electrodes when they are working near equilibrium, i.e., at low local overpotentials in order to determine, from local overpotentials measurements, the conditions in which the electrode is working as a 2 or 3-dimensional electrode and to compare the results with theory.

Trainham and Newman (1977)[25] developed a mathematical model for flow-through porous electrodes operating above and below the limiting current for a specific application to metal-ion removal from dilute streams. The model assumes that there is one primary reactant species in an excess of supporting electrolyte and that a simultaneous side reaction may occur.

Gaunand, Hutin, and Coeuret (1977)[26] investigated experimentally the metal solution potential distribution within flow-through fixed electrode under limiting current conditions for a solution of about 0.001 M potassium ferricyanide in 0.75 N sodium hydroxide electrolyte. They examined bed heights of 1 and 2 cm, the bed particles they used was consists of graphite spherical particles plated with nikel and gold respectively. They compared their results with a theoretical model which was in agreement with the experimental results.

Olive and Lacoste (1979) [15] studied experimentally the mass transfer in an electrochemical reactor for the recuperation of metal in industrial effluents (recovery of copper) from electrolyte solution of cupric sulfate and sulfuric acid, using a flow-through porous electrode technique working under limiting current conditions (see the comparison in chapter five). They suggested the correlation:

$$Sh = 4.3 Re_b^{0.35} Sc^{0.25} ,$$

for Reynolds numbers between 0.1 and 3.

Risch and Newman (1984) [14] made a theoretical comparison between flow-through and flow-by configuration at limiting current using the maximum solution-phase potential difference as basis for comparison. They concluded that at low conversions, a flow-by electrode is favorable, providing it can be constructed with length-to-width ratio greater than one. At high conversions, however a flow-by electrode is favorable if the ratio of the electrode width and penetration depth is less than 2.218.

Lahurd (1985) [27] suggested the voltage balance (VOLBAL) model, which is based upon the overall local voltage balance across single cell and is a one-dimensional simulation easily modified for different types of electrochemical reactors (flat plate, porous electrodes). She compared her model with a rigorous two-dimensional model suggested by White.

Bertazzoli and co-workers (1997)[20] presented an electrolytic cell with a porous cathode of reticulated vitreous carbon (RVC) designed to remove metals from aqueous streams by flowing simulated effluent metal ion containing through porous cathodes.

Masliy and Poddubny (1997)[18, 19] presented a mathematical simulation of a flow-through porous electrode operation on the basis of a one-dimensional model with a uniform conducting matrix and a cathodic process involving the main and side reaction (i.e. hydrogen evolution); they first considered the case of constant metal electrical conductivity then variable metal electrical conductivity.

Al-Habobi and Slaiman (2000) [28] performed experimental study of flow-through porous electrode of fixed bed of highly conductive copper particles for the reduction of Ti^{+4} (or Fe^{+3}) ions in the presence of sulfuric acid as a supporting electrolyte. They proposed a method to find the current efficiency experimentally by following the solution potential with time. They found that Ti^{+4} is slightly more efficient than Fe^{+3} as a redox system (the maximum efficiency is 86% for Ti^{+4}/Ti^{+3} , while it is 84% for Fe^{+3}/Fe^{+2}). They also found that mass transfer coefficient, for single particle, is directly proportional to $Re_b^{0.5-0.525}$ in the range of $16 < Re_b < 111$.

Abdul-Masih, Slaiman, and Sulaymon (2001) [29] studied a porous electrochemical reactor in which electrolyte and current flows in an axial direction, flow-through configuration. The cathode consists of fixed bed of highly conductive copper particles, working under limiting current conditions. Studying the cathodic reduction of ferric ions in the presence of sulfuric acid as a supporting electrolyte. They obtained the following correlation for mass transfer coefficient:

$$Sh = 2.255 Re_b^{0.452} Sc^{0.276}$$

for $55.7 < Re_b < 347.3$ and $1024 < Sc < 1715$.

They also developed a mathematical model and compared with experimental potential distributions, the results show good agreement between experimental and predicted potential distribution. Using the mathematical model equations and the correlation coming from the mass transfer study, a design equations have been proposed to relate the following parameters: yield, Reynolds number and the characteristic number of the studied system.

Hunsom and workers (2002)[30] described the effect of parameters (current intensity, pulse frequency, cathode type and flow rate of solution) on copper recovery in 3PE reactor constructed of graphite bed particles and a counter electrode made of titanium coated with ruthenium oxide. They obtained the optimum current density applied and optimum pulse frequency and they used a synthetic solution.

2.19 Scope of Present Work

The limitations of this work are presented as follows:

This work is devoted for studying a fixed one-dimensional porous electrode electrochemical reactor with ignoring radial changes of concentration, potential current density, flow-through electrode (electrolyte is passing in a direction parallel to the direction of the current and against it and flow is called counter flow), the electrochemical reaction studied is the deposition of copper from electrolyte solution of cupric sulfate and sulfuric acid and assuming no side reaction occurs, region of polarization curve studied is the mass transfer controlled region, conduction within electrolyte and metal phases obey Ohm's law, neglecting migration effects, hydrodynamics of flow are assumed to be plug flow, the mass transfer coefficient is assumed constant along the bed, operating temperature is 25°C, and electrolysis is done under steady state.

The aim of this work is to study the followings:

1. Simulation and design of an electrochemical reactor for the removal of copper ions for waste streams.
2. The concentration variation with distance (inside porous cathode).
3. The current changing (current in solution phase) with distance.
4. The reaction rate with distance.
5. The cathode potential variation with distance.

'Chapter Three

Mathematical Model and Electrochemical Reactor Design

3.9 Introduction

This chapter is dealing with three categories, the first one is theory of the packed bed electrochemical reactor and its use in heavy metal ion removal process and the second category is dealing with the simulation of the packed electrochemical reactor under mass transfer control and finally the third one deals with the design of the simulated electrochemical reactor.

3.10 Application of Packed Bed Electrochemical Reactors in Electrodeposition Processes

Different types of porous electrochemical reactors are used in the electrodeposition processes and that is because of their high efficiency, high conversion. They are classified according to the packing type and operation mode fixed or fluidized bed.

3.10.1 Fixed Bed Electrochemical Reactor

This type of packed bed reactors consists of a column containing the cathode (packed bed or working electrode) and anode (counter electrode) placed above the cathode. The anode may be of different types (perforated plate, or another packed bed). In present work the anodic reactions were discarded because the anode is not affecting the kinetics of the cathode but it is just a current source. The electrolyte solution is flowing upwards from the upstream (current feeder) through the lower hole of the column passing through the cathode where the reaction is occurring, then the electrolyte solution leaves the cathode and penetrates the anode to leave the reactor at the downstream. Fig. 3.1 demonstrates the fixed bed electrochemical reactor features.

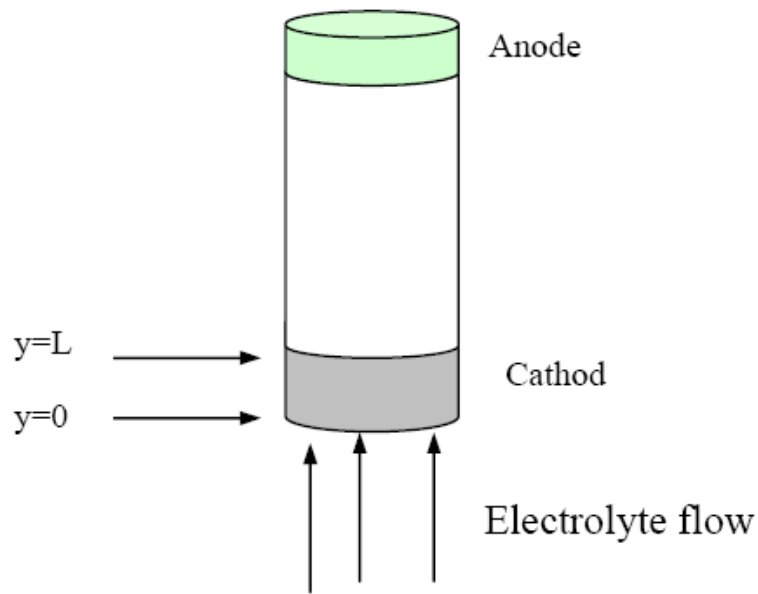


Figure 3.1 Schematic diagram of the porous electrode reactor to be simulated in present work

3.10.2 Pulsed Porous Percolated Reactor or(3PE Reactor)

The 3PE reactor can be considered as a compromise between fixed and fluidized bed reactors. It is composed of four components [30]:

- 1 A solid matrix composed of particles that act as voluminal cathode in contact with the current feeder.
- 2 A counter electrode or anode having a small geometrical surface area, the material used must be resistant to oxidizing conditions(platinum or titanium coated with ruthenium oxide are good choice)
- 3 A circulation pump is used to circulate the electrolyte in the system through the granular bed, tow advantages of this are the renewal of solution around the particles and structural improvement of the matel layer deposited.
- 4 A pulsating system creates movement of the granular bed in the reactor forcing the movement of metal-coated particles to the bottom of the bed and avoiding the problem of clogging.

3.10.3 The Porous Cathode of Reticulated Vitreous Carbon (RVC) Reactor

The RVC reactor is used for materials having the following properties

- 1 Chemically and electrochemically inert over a wide range of potentials and on a wide range of chemicals.
- 2 Has a high surface area within the porous structure that is accessible to electrochemically active species

- 3 Has a high fluid permeability
- 4 Is easily shaped as required by cell design considerations and has good mechanical resistance [31].

3.10.4 Kinetic Parameters

The most important kinetic parameter needed to represent in present work is the mass transport of copper ions through the electrolyte to the packing particles of the cathode. Reconsidering the simple general electrochemical reaction:

The mechanism of mass transfer is occurring as in the following steps.

1. Mass transfer (e.g., of O from the bulk solution to the electrode surface).
2. Electron transfer at the electrode surface.
3. Chemical reactions proceeding or following the electron transfer. These might be homogeneous processes, such as protonization, or dimerization, or heterogeneous, such as catalytic decomposition on the electrode surface.
4. Other surface reactions, such as adsorption, desorption, or crystallization (electrodeposition). **Fig. 3.2** illustrates the above steps schematically

The simplest reactions involve only mass transfer of a reactant to the electrode, heterogeneous electron transfer involving non-adsorbed species and mass transfer of the product to the bulk solution. More complex reaction sequences involving a series of electron transfers and protonations, branching mechanisms, parallel paths, or modifications of the electrode surface are quite common. When a steady-state current is obtained, the rates of the all reaction steps are the same. The magnitude of this current is often limited by the inherent sluggishness of one or more reactions called *rate-determining steps*.

The more facile reactions are then held back from maximum rates by the slowness with which such a step disposed of their products or creates their participants [12].

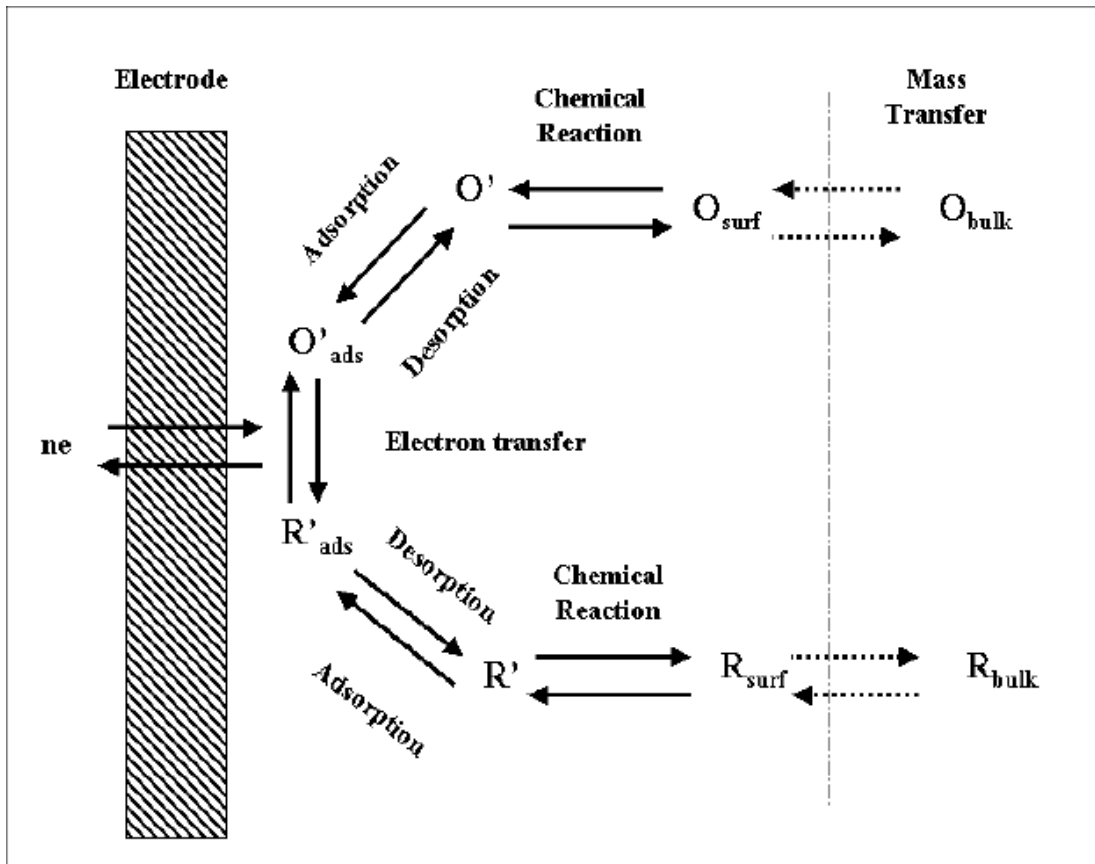


Figure 3.2 Mechanism of mass transport of ions [12]

Many workers have attempted to model convective mass transfer in packed beds by considering an isolated particle and the flow field around it. Although theoretical predictions have a common analytical form the most useful information is that obtained experimentally. Particularly relevant are the data Jolls and Hanratty [32] obtained electrochemically from a single sphere in a randomly packed bed. They found that: -

$$\frac{k_{av}d}{D} = 1.44 \left(\frac{\rho u d}{\mu} \right)^{0.58} \left(\frac{\mu}{\rho D} \right)^{1/3} \quad \dots(3.1)$$

Where d is the particle diameter and u is the superficial velocity based on the empty cross section of the bed. Equation (3.1) applies for Reynolds numbers between 35 and 142. Above $Re = 142$ they recommended alteration of the constant to 1.59 and the Reynolds number power to 0.56. Equation (3.5) corresponds to non-electrochemical packed bed data.

The most reliable estimate of the rate of mass transfer in a packed bed appears to be that obtained by Yip [33] for $Re < 0.1$ with 5/32 inch diameter spherical particles

$$\frac{k_{av}d}{D} = \frac{1.09}{\varepsilon} \left(\frac{\rho u d}{\mu} \right)^{1/3} \left(\frac{\mu}{\rho D} \right)^{1/3} \quad \dots(3.2)$$

where ε is the porosity and the one-third power on Re in equation (3.3) is indicative of Stokes flow. For higher flows a Reynolds number power of one half would be anticipated. Correlations for packed beds in the range $0.1 < Re < 23$ are not evident in the literature.

Hunsom [30] and workers obtained an empirical correlation for the mass transfer coefficient to be

$$\frac{k_{av}d}{D} = 1.2 \left(\frac{\rho u d}{\mu} \right)^{0.411} \left(\frac{\mu}{\rho D} \right)^{0.25} \quad \dots(3.3)$$

for Re between 6 and 16 and $Sc = 1568$.

For packed bed electrochemical reactor that is operated for recovery of heavy metals the most preferred correlations in many similar works are the Wilson and Geankoplis [34] correlations [23, 24] because of the fact that in electrodeposition process the porosity of the bed (cathode) decreasing and since

these correlations account the porosity as a variable so they are preferred to use as shown below.

$$\frac{k}{u} = \frac{0.4548}{\varepsilon} Re^{-0.4069} Sc^{-2/3} \quad \dots(3.4)$$

valid for Reynolds number between 10 and 1500

$$\frac{k}{u} = \frac{1.09}{\varepsilon} Re^{-2/3} Sc^{-2/3} \quad \dots(3.5)$$

valid for $0.0016 < Re < 55$ and $165 < Sc < 70600$

$$\frac{k}{u} = \frac{0.25}{\varepsilon} Re^{-0.31} Sc^{-2/3} \quad \dots(3.6)$$

valid for $55 < Re < 1500$ and $165 < Sc < 10690$.

3.11 Simulation of Electrochemical Processes

Electrochemical processes are complex because they involve many different simultaneous phenomena during the passage of an electrical current. Conduct of electrolysis brings about, for example, charge transfer within the double layer region, structural variation of electrode surface, ohmic resistance effects, and mass transport limitations of reactants and products to name a few. The relative importance of such processes depends upon the geometry and current density. Because the reaction rate along the surface is generally not uniform, the relative importance of such processes can therefore vary strongly within a cell [35].

In order to perform a theoretical analysis of such a complex problem, it is necessary to establish a model that accounts for essential features of an actual electrode without going into exact geometric details. Furthermore, the model

should be described by parameters, which can be obtained by suitably simple physical measurements. For example, a porous material of arbitrary random structure can be characterized by its porosity, average surface area per unit volume, volume average resistivity, etc. [15].

In this simulation three main categories will be simulated, first is the physical parameters (porosity changes, pressure drop), physical properties, and the third category is the kinetics modeling which are concentration distribution, current distribution, potential and reaction rate.

3.11.1 Porosity Change Inside Packed Bed

For spherical particles the equation that describe the change of porosity with particle and reactor diameters is given by Furnas (1993) [36].

$$\varepsilon = 0.375 + 0.34 \frac{d}{D_R} \quad \dots(3.7)$$

where

d : is the particle diameter

D_R: is the bed diameter

3.11.2 Physical Properties

Physical properties used are obtained from literature; since there are no explicit correlations for these properties therefore curve fitting is needed. The temperature is kept constant at 25°C (isothermal operation), therefore the

following properties are function of molar concentration for both cupric sulfate and sulfuric acid.

3.11.2.1 Diffusion Coefficient

Using the modified form of Stokes-Einstein equation given in [37]:

$$\frac{D\mu^{0.74}}{T} = Constant \quad \dots(3.8)$$

Since the operation is isothermal (constant temperature) the above equation is rewritten as $D\mu^{0.74} = constant$. The constant value must be evaluated. Hunsom et al (2002) [30] evaluated the diffusion coefficient (D) and viscosity at 25C^o for electrolyte consists of sulfuric acid and copperic sulfate to be as follows:

$$D = 5.89 \times 10^{-10} \text{ m}^2 / \text{s} \text{ and } \mu = 9.29 \times 10^{-4} \text{ kg/m s.}$$

The constant value will be 3.36×10^{-12} , therefore the relation will be

$$D = \frac{3.36 \times 10^{-12}}{\mu^{0.74}} \quad \dots(3.9)$$

3.11.3 Mathematical Modeling

The kinetic parameters in this simulation are for a specified region in the polarization curve that is mass transfer controlled process.

Using the general mass balance equation as follows [9]:

$$D \frac{d^2 C_b}{dx^2} - u \frac{dC_b}{dx} = ak(C_b - C_s) \quad \dots(3.10)$$

The surface concentration in the mass balance equation for the case of mass transfer controlled is equal to zero so that equation (3.10) will be reduced to the following form

$$D \frac{d^2 C_b}{dx^2} - u \frac{dC_b}{dx} - akC_b = 0 \quad \dots(3.11)$$

equation (3.11) is a second order linear differential equation which may be solved by the method of inverse operator

using the proportionality between the change current density in the solution phase and the quantity passed due to electricity in [9]

$$\frac{di_s}{dx} = uzF \frac{dC_b}{dx} \quad \dots(3.12)$$

So solving equation (3.11) and obtaining the first derivative for the bulk concentration in order to obtain an expression for the solution current density (i_s) The current in the metal phase is found from the following current balance

$$I = i_s + i_m \quad \dots(3.13)$$

Applying Ohm's law on both solution and metal phases as follows [21]:

$$i_s = -\kappa \frac{d\phi_s}{dx} \quad \dots(3.15)$$

$$i_m = -\sigma \frac{d\phi_m}{dx} \quad \dots(3.16)$$

equations (3.11) through (3.16) may be solved with the following boundary conditions to obtain the distributions for the concentration , current , and potential.

$$\text{BC. 1 at } x = 0, C_b = C_f, i_s = 0, \phi_s \approx 0.$$

BC. 2 at $x = L$, $i_s = I$

3.12 Solution of Equations

The mass balance equation, equation (3.11), is solved by the method of inverse operator as follows:

$$Dm^2 - um - ak = 0 \quad \dots(3.17)$$

the roots of equation (3.17) are found to be

$$m = \frac{u \pm \sqrt{u^2 + 4akD}}{2D} \quad \dots(3.18)$$

the general solution of equation (3.11) is

$$C_b = C_1 e^{m_1 x} + C_2 e^{m_2 x} \quad \dots(3.19)$$

neglecting the root with the positive ve, because it leads to unstable profile for the concentration, and substitution of equation (3.18) into the general solution (3.19)

$$C_b = C_1 \exp\left(\frac{u - \sqrt{u^2 + 4akD}}{2D} x\right) \quad \dots(3.20)$$

applying BC. 1 to get

$$C_b = C_f e^{mx} \quad \dots(3.21)$$

where m is defined as follows:

$$m = \frac{u - \sqrt{u^2 + 4akD}}{2D} \quad \dots(3.22)$$

substituting the first derivative of equation (3.21) into equation (3.12)

$$\frac{di_s}{dx} = uzFC_f e^{mx} \quad \dots(3.23)$$

integrating equation (3.23) using BC. 1

$$i_s = uzFC_f e^{mx} + C_1 \quad \dots(3.24)$$

the expression for the solution current density is as follows:

$$i_s = uzFC_f (e^{mx} - 1) \quad \dots(3.25)$$

defining the cathode potential (E) to be the difference between the metal potential and solution potential, i. e. $\phi_m - \phi_s$.

$$E = \int \left(\frac{d\phi_m}{dx} - \frac{d\phi_s}{dx} \right) dx \quad \dots(3.26)$$

$$\frac{dE}{dx} = \frac{d\phi_m}{dx} - \frac{d\phi_s}{dx} = -\frac{i_m}{\sigma} + \frac{i_s}{\kappa} \quad \dots(3.27)$$

introducing the current balance equation (3.13) leads to

$$\frac{dE}{dx} = i_s \left(\frac{1}{\kappa} + \frac{1}{\sigma} \right) - \frac{I}{\sigma} \quad \dots(3.28)$$

$$E = \int \left\{ i_s \left(\frac{1}{\kappa} + \frac{1}{\sigma} \right) - \frac{I}{\sigma} \right\} dx \quad \dots(3.29)$$

$$E = \int_0^x \left\{ \left[uzFC_f (e^{mx} - 1) \right] \left(\frac{1}{\kappa} + \frac{1}{\sigma} \right) - \frac{I}{\sigma} \right\} dx \quad \dots(3.30)$$

Assuming the reciprocal of metal conductivity (σ) to be approximately zero, i.e. very high conductivity so that equation (3.30) is simplified as follows:

$$E = \int_0^x \left\{ \left[\frac{uzFC_f}{\kappa} (e^{mx} - 1) \right] \right\} dx \quad \dots(3.31)$$

integrating equation (3.31) leads to

$$E(x) = \frac{uzFC_f}{m\kappa} (e^{mx} - mx) + C_2 \quad \dots(3.32)$$

the cathode potential cannot be evaluated at the bed inlet and outlet because there is no mathematical expression for the cathode potential therefore equation (3.32) is replaced in terms of $E(L)$, i.e. potential at the outlet so that

$$E(L) = \frac{uzFC_f}{m\kappa} (e^{mL} - mL) + C_2 \quad \dots(3.33)$$

subtracting equation (3.32) from (3.33) leads to

$$E(x) - E(L) = \frac{uzFC_f}{m\kappa} [e^{mx} - e^{mL} + m(L - x)] \quad \dots(3.34)$$

where equation (3.34) represents the cathode potential distribution

the local limiting current (i_L) is given by the following

$$i_L(x) = zFk C_b(x) \quad \dots(3.35)$$

substituting equation (3.21) into equation (3.35)

$$i_L(x) = zFk C_f e^{mx} \quad \dots(3.36)$$

the total limiting current density (I_L) is given by integrating the local limiting current density (equation (3.36)) for the whole bed as follows [19]

$$I_L = \int_0^L a \cdot i_L dx \quad \dots(3.37)$$

$$I_L = \frac{azFkC_f}{m} (e^{mL} - 1) \quad \dots(3.38)$$

3.13 Electrochemical Reactor Design

The designs of electrochemical reactors are almost as varied as are the applications of electrochemical technology. Specific and unique cell designs and reactor configurations are the norm for the various types of batteries, fuel cells and electrosynthesis processes [38].

Electrochemical reactor design has been largely untouched by chemical engineering at a fundamental level. Many of the large-scale electrochemical processes such as the manufacture of chlorine or aluminum have been in existence for more than eighty years in forms which are not too dissimilar to those of the present day [9].

With the majority of electrochemical processes only one of the electrode reactions gives a desirable product, so that the reaction that occurs at the counter-electrode has a status comparable with the rate of a side reaction in conventional chemical process.

In a number of cases the two electrode reactions proceed more or less independently except that their reaction rates are coupled. That is to say that the change in the environment which attends either of the reactions has little effect on the progress of the other. If this situation exists, then most of the reactor design can be accomplished by considering the course of the desired reaction alone. Little more attention need to be paid to the second reaction other than to assess its voltage requirement.

The partial separation of the electrode processes, which is thus possible, forms the basis of most of the design methods in the literatures. It is appropriate to all types of single-compartment reactors and to two-compartment reactors which contain a diaphragm [9, 39].

The complexity of a porous electrode is easily envisaged from the one-dimensional sketch in **Figure 3.3**

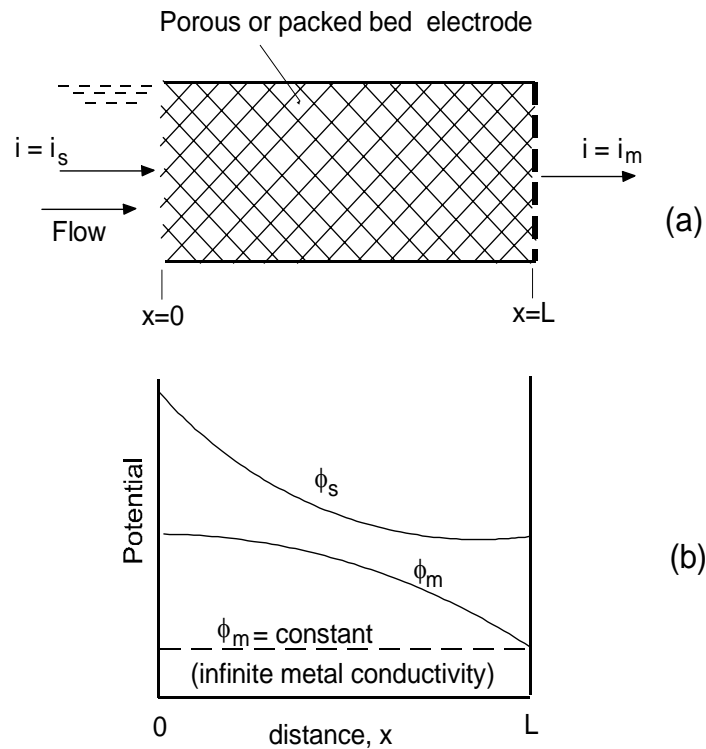


Figure 3.3 One-dimensional porous cathode [9].

- a. Current and solution paths. (b) Solution and metal potential distributions along the electrode

The total electric charge passing through the electrode normal to the flow is constant from continuity consideration. However, the charge carried through each phase varies with position inside the electrode. At the bulk solution/electrode interface ($x=0$) current starts to flow in the metal and, at the collector, ($x=L$), all the current flows in the metal. Although the potential of the metal decreases in absolute magnitude along the electrode in the direction of the collector, this change is small compared with the fall in the solution potential. The latter is due to the progressively greater paths associated with ionic transfer through the electrode. Typical potential distributions for both solution and metal are shown for a porous cathode in Fig. 3.3. At the front end, where the superficial current (i.e. the current based on unit cross-sectional area of the electrode) resides in the solution, the solution potential gradient has its greater magnitude. At the back end the reverse situation applies and the metal potential gradient has its greatest value [9].

3.13.1 Stepwise Procedure For Electrochemical Cell Design

MacMullin instructs us always to visualize the final plant during development, and to visualize alternatives in cell and process arrangement during the design stage. Table 3.1 presents the stepwise procedure for cell design; points 3, 5, 6, 12 and possibly 13 require input from pilot-plant scale elements [40].

Table 3.1 Stepwise procedure for electrochemical cell design [40].

1.	Overall reaction and electrode reactions.
2.	Analyze polarization data (i_o , i_L).
3.	Analyze current efficiency as a function of i .
4.	Specify requirements diaphragm.

5.	Cell input/output table and anolyte/catholyte balances.
6.	Preliminary material balance.
7.	Anode and cathode material selection.
8.	Diaphragm selection.
9.	Tank and cover materials.
10.	Cell geometry.
11.	Preliminary dimensional drawing.
12.	Voltage balances at various i .
13.	Heat balances at various i .
14.	Cost estimation.
15.	Vary size and repeat.

Chapter Four

Results and Interpretations

The purpose of this study is to build a simple model to predict the behavior of fixed bed electrochemical reactor at different operating parameters like feed concentrations, feed flow rate, bed thickness, and operating under mass transfer control process.

In this chapter the parameters mentioned above and their ranges are outlined, simulation input variables classified as groups are also outlined with results of simulation runs.

4.5 The Studied Parameters in Present Work

- Concentration of the feed electrolyte was 0.5 M H_2SO_4 and 0.001 and 0.01 M CuSO_4
- Range of polarization curve studied is the mass transfer control region
- Electrolyte volumetric flow rates are 300, 500, 700 and 1000 L / h
- Packing particles of spherical shape of diameter 4 mm
- Bed of a 4 cm diameter and of thickness 2, 3, and 4 cm

The following effect of flow rate, feed concentration of copperic sulfate, bed thickness on the concentration distribution, reaction rate, potential distribution, and current density distribution.

4.6 Effect of Flow Rate

The effect of flow rate is presented in the following tables on the concentration distribution, reaction rate, potential distribution, and current density distribution.

4.6.1 Concentration Distribution

Tables (4.1–4.3) and tables A.1-A.3 (see Appendix A) represent the effect of flow rate on the concentration distribution given by equation (3.21).

Table 4.1 Effect of flow rate on the concentration distribution in M for bed thickness of 2 cm, feed concentration 0.001 M

x (m)	300 L / h	500 L / h	700 L / h	1000 L / h
0.000	0.001	0.001	0.001	0.001
0.002	0.00099883	0.000999	0.0009991	0.00099919
0.004	0.00099765	0.000998	0.00099819	0.00099838
0.006	0.00099648	0.000997	0.00099729	0.00099758
0.008	0.00099531	0.000996	0.00099639	0.00099677
0.010	0.00099414	0.000995	0.00099549	0.00099596
0.012	0.00099297	0.000994	0.00099459	0.00099516
0.014	0.00099181	0.000993	0.00099369	0.00099435
0.016	0.00099064	0.00099201	0.0009928	0.00099355
0.018	0.00098948	0.00099101	0.0009919	0.00099274
0.020	0.00098832	0.00099002	0.000991	0.00099194

Table 4.2 Effect of flow rate on the concentration distribution in M for bed thickness of 3 cm, feed concentration 0.001 M

x (m)	300 L / h	500 L / h	700 L / h	1000 L / h
0.000	0.001	0.001	0.001	0.001
0.003	0.00099824	0.0009985	0.00099865	0.00099879
0.006	0.00099648	0.000997	0.00099729	0.00099758
0.009	0.00099473	0.0009955	0.00099594	0.00099637
0.012	0.00099297	0.000994	0.00099459	0.00099516
0.015	0.00099123	0.00099251	0.00099325	0.00099395
0.018	0.00098948	0.00099101	0.0009919	0.00099274
0.021	0.00098774	0.00098952	0.00099056	0.00099154
0.024	0.000986	0.00098804	0.00098921	0.00099034
0.027	0.00098426	0.00098655	0.00098787	0.00098914
0.030	0.00098253	0.00098507	0.00098654	0.00098794

Table 4.3 Effect of flow rate on the concentration distribution in M for bed thickness of 4 cm, feed concentration 0.001 M

x (m)	300 L / h	500 L / h	700 L / h	1000 L / h
0.000	0.001	0.001	0.001	0.001
0.004	0.00099765	0.000998	0.00099819	0.00099838
0.008	0.00099531	0.000996	0.00099639	0.00099677
0.012	0.00099297	0.000994	0.00099459	0.00099516
0.016	0.00099064	0.00099201	0.0009928	0.00099355
0.020	0.00098832	0.00099002	0.000991	0.00099194
0.024	0.000986	0.00098804	0.00098921	0.00099034
0.028	0.00098368	0.00098606	0.00098743	0.00098874
0.032	0.00098137	0.00098408	0.00098564	0.00098714
0.036	0.00097907	0.00098211	0.00098387	0.00098554
0.040	0.00097677	0.00098014	0.00098209	0.00098395

Examining tables 4.1–4.3 and tables A.1-A.3 leads to the interpretation that as flow rate increases the downstream concentration increases which causes the conversion to be increased when flow rate decreases although the change in concentration is finite. Tables A.1-A.3 (copperic sulfate concentration 0.01) as well show the same behavior.

4.6.2 Reaction rate Distribution

Tables (4.4–4.6) and tables (A.4-A.6) represent the effect of flow rate on the reaction rate founded by using equation (3.36).

Table 4.4 Effect of flow rate on the reaction rate distribution (A/m^2) for bed thickness of 2 cm, feed concentration 0.001 M

x (m)	300 L / h	500 L / h	700 L / h	1000 L / h
0.000	8.4818769	12.066119	15.219344	19.466071
0.002	8.4719153	12.054022	15.205597	19.450327
0.004	8.4619653	12.041937	15.191862	19.434596
0.006	8.4520271	12.029865	15.17814	19.418878
0.008	8.4421006	12.017805	15.164429	19.403173
0.010	8.4321857	12.005756	15.150732	19.38748
0.012	8.4222824	11.99372	15.137046	19.3718
0.014	8.4123908	11.981696	15.123373	19.356133
0.016	8.4025108	11.969684	15.109712	19.340478
0.018	8.3926424	11.957683	15.096064	19.324836
0.020	8.3827855	11.945695	15.082428	19.309207

Table 4.5 Effect of flow rate on the reaction rate distribution (A/m^2) for bed thickness of 3 cm, feed concentration 0.001 M

x (m)	300 L / h	500 L / h	700 L / h	1000 L / h
0.000	8.4818769	12.066119	15.219344	19.466071
0.003	8.4669388	12.047978	15.198728	19.44246
0.006	8.4520271	12.029865	15.17814	19.418878
0.009	8.4371416	12.011779	15.157579	19.395325
0.012	8.4222824	11.99372	15.137046	19.3718
0.015	8.4074493	11.975688	15.116541	19.348304
0.018	8.3926424	11.957683	15.096064	19.324836
0.021	8.3778615	11.939706	15.075615	19.301397
0.024	8.3631066	11.921755	15.055193	19.277986
0.027	8.3483778	11.903832	15.034799	19.254604
0.030	8.3336749	11.885935	15.014433	19.23125

Table 4.6 Effect of flow rate on the reaction rate distribution (A/m^2) for bed thickness of 4 cm, feed concentration 0.001 M

x (m)	300 L / h	500 L / h	700 L / h	1000 L / h
0.000	8.4818769	12.066119	15.219344	19.466071
0.004	8.4619653	12.041937	15.191862	19.434596
0.008	8.4421006	12.017805	15.164429	19.403173
0.012	8.4222824	11.99372	15.137046	19.3718
0.016	8.4025108	11.969684	15.109712	19.340478
0.020	8.3827855	11.945695	15.082428	19.309207
0.024	8.3631066	11.921755	15.055193	19.277986
0.028	8.3434739	11.897863	15.028007	19.246816
0.032	8.3238873	11.874019	15.00087	19.215696
0.036	8.3043466	11.850223	14.973782	19.184626
0.040	8.2848519	11.826474	14.946743	19.153607

Tables 4.4–4.6 and tables A.4-A.6 demonstrating a behavior such that as flow rate increases the reaction rate increases and when increasing copperic sulfate concentration to 0.01M also the same behavior is noticed.

4.6.3 Potential Distribution

Tables (4.7–4.9) and tables (A.7-A.9) represent the effect of flow rate on the potential distribution founded by equation (3.34).

Table 4.7 Effect of flow rate on the potential distribution (V) for bed thickness of 2 cm, feed concentration 0.001 M

x (m)	300 L / h	500 L / h	700 L / h	1000 L / h
0.000	0.0674187	0.095963197	0.121081186	0.154915809
0.002	0.066742134	0.095000676	0.11986709	0.153362889
0.004	0.064713498	0.092114399	0.116226264	0.148705804
0.006	0.061334378	0.087306294	0.110160899	0.140947063
0.008	0.05660636	0.080578289	0.101673187	0.130089176
0.010	0.05053103	0.071932308	0.090765315	0.116134649
0.012	0.043109969	0.061370275	0.077439469	0.099085986
0.014	0.034344758	0.048894109	0.061697834	0.078945691
0.016	0.024236975	0.03450573	0.04354259	0.055716263
0.018	0.012788197	0.018207055	0.02297592	0.0294002
0.020	0	0	0	0

Table 4.8 Effect of flow rate on the potential distribution (V) for bed thickness of 3 cm, feed concentration 0.001 M

x (m)	300 L / h	500 L / h	700 L / h	1000 L / h
0.000	0.151395989	0.21555729	0.272023423	0.348091646
0.003	0.149874015	0.213391979	0.269292118	0.344598047
0.006	0.145311667	0.206900387	0.261103136	0.3341229
0.009	0.1377143	0.196089019	0.247463871	0.316674673
0.012	0.127087258	0.180964368	0.228381706	0.292261823
0.015	0.113435878	0.161532919	0.203864014	0.260892799
0.018	0.096765487	0.137801149	0.173918157	0.222576037
0.021	0.0770814	0.109775521	0.138551489	0.177319965
0.024	0.054388926	0.077462491	0.097771353	0.125132998
0.027	0.028693363	0.040868505	0.051585082	0.066023545
0.030	0	0	0	0

Table 4.9 Effect of flow rate on the potential distribution (V) for bed thickness of 4 cm, feed concentration 0.001 M

x (m)	300 L / h	500 L / h	700 L / h	1000 L / h
0.000	0.268623593	0.382574732	0.482871289	0.617997632
0.004	0.265918391	0.378725934	0.478016366	0.611787626
0.008	0.257811253	0.367189824	0.46346329	0.593170998
0.012	0.244314862	0.34798181	0.439229572	0.562167809
0.016	0.225441868	0.321117265	0.405332693	0.518798085
0.020	0.201204893	0.286611535	0.361790103	0.463081823
0.024	0.17161653	0.244479933	0.308619218	0.395038984
0.028	0.13668934	0.194737741	0.245837427	0.3146895
0.032	0.096435858	0.137400213	0.173462083	0.222053269
0.036	0.050868586	0.072482568	0.09151051	0.117150158
0.040	0	0	0	0

The cathode potential presented in Tables 4.7–4.9 and tables A.7-A.9 was expressed as the difference between upstream and downstream but it still give an impression for the absolute values of the cathode potential to be in a decreasing manner along the bed.

The cathode potential increases when flow increases as concentration and bed length increases.

4.6.4 Solution Current Density Distribution

Tables (4.10–4.11) represent the effect of flow rate on the solution current density distribution founded by equation (3.25).

Table 4.10 Effect of flow rate on the solution current density distribution in (A/m^2) for bed thickness of 2 cm, feed concentration 0.001 M

x (m)	300 L / h	500 L / h	700 L / h	1000 L / h
0.000	0	0	0	0
0.002	15.0295348	21.3825031	26.9717095	34.4993841
0.004	30.0414181	42.7435694	53.919056	68.9708661
0.006	45.0356705	64.0832204	80.8420613	103.414469
0.008	60.0123128	85.4014775	107.740748	137.830214
0.010	74.9713656	106.698362	134.615137	172.218125
0.012	89.9128497	127.973896	161.465251	206.578225
0.014	104.836786	149.2281	188.291111	240.910534
0.016	119.743194	170.460996	215.092741	275.215077
0.018	134.632095	191.672605	241.87016	309.491876
0.020	149.50351	212.862948	268.623393	343.740952

Table 4.11 Effect of flow rate on the solution current density distribution in (A/m^2) for bed thickness of 3 cm, feed concentration 0.001 M

x (m)	300 L / h	500 L / h	700 L / h	1000 L / h
0.000	0	0	0	0
0.003	22.5376816	32.0657145	40.4484268	51.7386114
0.006	45.0356705	64.0832204	80.8420613	103.414469
0.009	67.4940366	96.05259	121.180978	155.027648
0.012	89.9128497	127.973896	161.465251	206.578225
0.015	112.292179	159.84721	201.694953	258.066275
0.018	134.632095	191.672605	241.87016	309.491876
0.021	156.932667	223.450152	281.990945	360.855102
0.024	179.193963	255.179924	322.057382	412.156028
0.027	201.416053	286.861992	362.069543	463.394732
0.030	223.599007	318.496429	402.027504	514.571288

The relation between the solution current density and flow rate is similar to that between reaction rate and flow rate except that the solution current density is increasing with distance starts from zero to total applied limiting current density.

4.7 Effect of Cupric Sulfate Feed Concentration

The effect of cupric sulfate feed concentration is presented in the followings on the concentration distribution, reaction rate, potential distribution, and current density distribution.

4.7.1 Concentration Distribution

Tables (4.12–4.15) and tables (A.10-A.11) give the effect of cupric sulfate feed concentration on the concentration distribution for different bed thickness and flow rates.

Table 4.12 Effect of cupric sulfate concentration on the concentration distribution in (M) for bed thickness of 2 cm, and flow rates 300 and 500 L / h

x (m)	0.001 M		0.01 M	
	300 L / h	500 L / h	300 L / h	500 L / h
0.000	0.001	0.001	0.01	0.01
0.002	0.00099883	0.000999	0.00998833	0.00999004
0.004	0.00099765	0.000998	0.00997668	0.00998009
0.006	0.00099648	0.000997	0.00996504	0.00997016
0.008	0.00099531	0.000996	0.00995342	0.00996023
0.010	0.00099414	0.000995	0.00994181	0.00995031
0.012	0.00099297	0.000994	0.00993021	0.0099404
0.014	0.00099181	0.000993	0.00991863	0.0099305
0.016	0.00099064	0.00099201	0.00990706	0.00992061
0.018	0.00098948	0.00099101	0.0098955	0.00991074
0.020	0.00098832	0.00099002	0.00988396	0.00990087

Table 4.13 Effect of cupric sulfate concentration on the concentration distribution in (M) for bed thickness of 2 cm, and flow rates 700 and 1000 L / h

x (m)	0.001 M		0.01 M	
	700 L / h	1000 L / h	700 L / h	1000 L / h
0.000	0.001	0.001	0.01	0.01
0.002	0.0009991	0.00099919	0.00999103	0.00999197
0.004	0.00099819	0.00099838	0.00998206	0.00998394
0.006	0.00099729	0.00099758	0.00997311	0.00997592
0.008	0.00099639	0.00099677	0.00996416	0.00996791
0.010	0.00099549	0.00099596	0.00995522	0.0099599
0.012	0.00099459	0.00099516	0.00994629	0.0099519
0.014	0.00099369	0.00099435	0.00993737	0.0099439
0.016	0.0009928	0.00099355	0.00992845	0.00993591
0.018	0.0009919	0.00099274	0.00991954	0.00992793
0.020	0.000991	0.00099194	0.00991064	0.00991996

Table 4.14 Effect of cupric sulfate concentration on the concentration distribution in (M) for bed thickness of 3 cm, and flow rates 300 and 500 L / h

x (m)	0.001 M		0.01 M	
	300 L / h	500 L / h	300 L / h	500 L / h
0.000	0.001	0.001	0.01	0.01
0.003	0.00099824	0.0009985	0.00998655	0.00998795
0.006	0.00099648	0.000997	0.00997311	0.00997592
0.009	0.00099473	0.0009955	0.00995969	0.0099639
0.012	0.00099297	0.000994	0.00994629	0.0099519
0.015	0.00099123	0.00099251	0.00993291	0.00993991
0.018	0.00098948	0.00099101	0.00991954	0.00992793
0.021	0.00098774	0.00098952	0.00990619	0.00991597
0.024	0.000986	0.00098804	0.00989287	0.00990403
0.027	0.00098426	0.00098655	0.00987956	0.00989209
0.030	0.00098253	0.00098507	0.00986626	0.00988018

Table 4.15 Effect of copperic sulfate concentration on the concentration distribution in (M) for bed thickness of 3 cm, and flow rates 700 and 1000 L / h

x (m)	0.001 M		0.01 M	
	700 L / h	1000 L / h	700 L / h	1000 L / h
0.000	0.001	0.001	0.01	0.01
0.003	0.00099865	0.00099879	0.00998655	0.00998795
0.006	0.00099729	0.00099758	0.00997311	0.00997592
0.009	0.00099594	0.00099637	0.00995969	0.0099639
0.012	0.00099459	0.00099516	0.00994629	0.0099519
0.015	0.00099325	0.00099395	0.00993291	0.00993991
0.018	0.0009919	0.00099274	0.00991954	0.00992793
0.021	0.00099056	0.00099154	0.00990619	0.00991597
0.024	0.00098921	0.00099034	0.00989287	0.00990403
0.027	0.00098787	0.00098914	0.00987956	0.00989209
0.030	0.00098654	0.00098794	0.00986626	0.00988018

The concentration distribution is affected by the change in copperic sulfate concentration from 0.001M to 0.01M in such a way that at high copperic sulfate concentration the conversion will be reduced so that the diluted solutions will experience a greater conversion to take place.

4.7.2 Reaction rate Distribution

Table 4.16 give the effect of copperic sulfate feed concentration on the reaction rate distribution for different bed thickness and flow rates.

Table 4.16 Effect of copperic sulfate concentration on the reaction rate distribution in (A/m^2) for bed thickness of 2 cm, and flow rates 300 and 500 L / h

x (m)	0.001 M		0.01 M	
	300 L / h	500 L / h	300 L / h	500 L / h
0.000	8.4818769	12.066119	84.246923	119.8477
0.002	8.4719153	12.054022	84.148646	119.72835
0.004	8.4619653	12.041937	84.050482	119.60913
0.006	8.4520271	12.029865	83.952434	119.49002
0.008	8.4421006	12.017805	83.854499	119.37104
0.010	8.4321857	12.005756	83.756679	119.25217
0.012	8.4222824	11.99372	83.658973	119.13342
0.014	8.4123908	11.981696	83.561381	119.01479
0.016	8.4025108	11.969684	83.463903	118.89628
0.018	8.3926424	11.957683	83.366539	118.77788
0.020	8.3827855	11.945695	83.269288	118.6596

It very clear from table 4.16 above that the reaction rate will increase significantly when copperic sulfate concentration increases and since this behavior is quite obvious there is no need to demonstrate reaction rate behaviour for other flow rates.

4.7.3 Potential Distribution

Table 4.17 give the effect of copperic sulfate feed concentration on the potential distribution for different bed thickness and flow rates.

Table 4.17 Effect of copperic sulfate concentration on the potential distribution in (V) for bed thickness of 2 cm, and flow rates 300 and 500 L / h

x (m)	0.001 M		0.01 M	
	300 L / h	500 L / h	300 L / h	500 L / h
0.000	0.0674187	0.095963197	0.682112361	0.970909132
0.002	0.066742134	0.095000676	0.675267336	0.961171005
0.004	0.064713498	0.092114399	0.654742908	0.931969554
0.006	0.061334378	0.087306294	0.620555035	0.883324161
0.008	0.05660636	0.080578289	0.572719656	0.815254187
0.010	0.05053103	0.071932308	0.511252691	0.727778976
0.012	0.043109969	0.061370275	0.436170043	0.62091785
0.014	0.034344758	0.048894109	0.347487594	0.494690114
0.016	0.024236975	0.03450573	0.245221209	0.349115053
0.018	0.012788197	0.018207055	0.129386735	0.184211933
0.020	0	0	0	0

The influence of copperic sulfate concentration on cathode potential is quite similar to that on reaction rate with the same significance.

4.7.4 Solution Current Density Distribution

Table 4.18 give the effect of cupric sulfate feed concentration on the solution current density distribution for different bed thickness and flow rates.

Table 4.18 Effect of cupric sulfate concentration on the solution current density distribution in (A/m^2) for bed thickness of 2 cm, and flow rates 300 and 500 L / h

x (m)	0.001 M		0.01 M	
	300 L / h	500 L / h	300 L / h	500 L / h
0.000	0	0	0	0
0.002	15.0295348	21.3825031	149.282655	212.384152
0.004	30.0414181	42.7435694	298.391165	424.556815
0.006	45.0356705	64.0832204	447.325732	636.5182
0.008	60.0123128	85.4014775	596.086561	848.268517
0.010	74.9713656	106.698362	744.673854	1059.80798
0.012	89.9128497	127.973896	893.087813	1271.13679
0.014	104.836786	149.2281	1041.32864	1482.25516
0.016	119.743194	170.460996	1189.39654	1693.1633
0.018	134.632095	191.672605	1337.29171	1903.86143
0.020	149.50351	212.862948	1485.01435	2114.34974

The solution current density is increases as cupric sulfate concentration is increased similarly to that for reaction rate and cathode potential.

4.8 Effect of Bed Thickness

4.8.1 Concentration Distribution

Tables (4.19_4.20) give the effect of bed thickness on the concentration distribution.

Table 4.19 Effect of Bed thickness on the concentration distribution in (M), flow rate 300 L / h and copperic sulfate concentrations 0.001 and 0.01M

X / L	2 cm		3 cm		4 cm	
	0.001 M	0.01 M	0.001 M	0.01 M	0.001 M	0.01 M
0	0.001	0.01	0.001	0.01	0.001	0.01
0.1	0.00099883	0.00998833	0.00099824	0.00998251	0.00099765	0.00997668
0.2	0.00099765	0.00997668	0.00099648	0.00996504	0.00099531	0.00995342
0.3	0.00099648	0.00996504	0.00099473	0.00994761	0.00099297	0.00993021
0.4	0.00099531	0.00995342	0.00099297	0.00993021	0.00099064	0.00990706
0.5	0.00099414	0.00994181	0.00099123	0.00991284	0.00098832	0.00988396
0.6	0.00099297	0.00993021	0.00098948	0.0098955	0.000986	0.00986091
0.7	0.00099181	0.00991863	0.00098774	0.00987819	0.00098368	0.00983792
0.8	0.00099064	0.00990706	0.000986	0.00986091	0.00098137	0.00981498
0.9	0.00098948	0.0098955	0.00098426	0.00984366	0.00097907	0.00979209
1	0.00098832	0.00988396	0.00098253	0.00982644	0.00097677	0.00976926

Table 4.20 Effect of Bed thickness on the concentration distribution flow rate in (M),
500 L / h and copperic sulfate concentrations 0.001 and 0.01M

X / L	2 cm		3 cm		4 cm	
	0.001 M	0.01 M	0.001 M	0.01 M	0.001 M	0.01 M
0	0.001	0.01	0.001	0.01	0.001	0.01
0.1	0.000999	0.00999004	0.0009985	0.00998507	0.000998	0.00998009
0.2	0.000998	0.00998009	0.000997	0.00997016	0.000996	0.00996023
0.3	0.000997	0.00997016	0.0009955	0.00995527	0.000994	0.0099404
0.4	0.000996	0.00996023	0.000994	0.0099404	0.00099201	0.00992061
0.5	0.000995	0.00995031	0.00099251	0.00992556	0.00099002	0.00990087
0.6	0.000994	0.0099404	0.00099101	0.00991074	0.00098804	0.00988116
0.7	0.000993	0.0099305	0.00098952	0.00989594	0.00098606	0.00986149
0.8	0.00099201	0.00992061	0.00098804	0.00988116	0.00098408	0.00984186
0.9	0.00099101	0.00991074	0.00098655	0.0098664	0.00098211	0.00982227
1	0.00099002	0.00990087	0.00098507	0.00985167	0.00098014	0.00980272

Table 4.19 and 4.20 show that the when bed thickness increases the downstream concentration will be reduced, i.e. the conversion increases.

4.8.2 Reaction Rate Distribution

Tables (4.21_4.22) give the effect of bed thickness on the reaction rate distribution.

Table 4.21 Effect of Bed thickness on the reaction rate distribution in (A/m^2), flow rate 300 L / h and cupric sulfate concentrations 0.001 and 0.01M

X / L	2 cm		3 cm		4 cm	
	0.001 M	0.01 M	0.001 M	0.01 M	0.001 M	0.01 M
0	8.4818769	84.24692	8.4818769	84.24692	8.4818769	84.24692
0.1	8.4719153	84.14865	8.4669388	84.09955	8.4619653	84.05048
0.2	8.4619653	84.05048	8.4520271	83.95243	8.4421006	83.8545
0.3	8.4520271	83.95243	8.4371416	83.80558	8.4222824	83.65897
0.4	8.4421006	83.8545	8.4222824	83.65897	8.4025108	83.4639
0.5	8.4321857	83.75668	8.4074493	83.51263	8.3827855	83.26929
0.6	8.4222824	83.65897	8.3926424	83.36654	8.3631066	83.07513
0.7	8.4123908	83.56138	8.3778615	83.22071	8.3434739	82.88142
0.8	8.4025108	83.4639	8.3631066	83.07513	8.3238873	82.68816
0.9	8.3926424	83.36654	8.3483778	82.9298	8.3043466	82.49535
1	8.3827855	83.26929	8.3336749	82.78473	8.2848519	82.303

Table 4.22 Effect of Bed thickness on the reaction rate distribution in (A/m^2), flow rate 500 L / h and cupric sulfate concentrations 0.001 and 0.01M

X / L	2 cm		3 cm		4 cm	
	0.001 M	0.01 M	0.001 M	0.01 M	0.001 M	0.01 M
0	12.06612	119.8477	12.06612	119.8477	12.06612	119.8477
0.1	12.05402	119.7284	12.04798	119.6687	12.04194	119.6091
0.2	12.04194	119.6091	12.02986	119.49	12.0178	119.371
0.3	12.02986	119.49	12.01178	119.3116	11.99372	119.1334
0.4	12.0178	119.371	11.99372	119.1334	11.96968	118.8963
0.5	12.00576	119.2522	11.97569	118.9555	11.9457	118.6596
0.6	11.99372	119.1334	11.95768	118.7779	11.92176	118.4234
0.7	11.9817	119.0148	11.93971	118.6005	11.89786	118.1877
0.8	11.96968	118.8963	11.92176	118.4234	11.87402	117.9524
0.9	11.95768	118.7779	11.90383	118.2466	11.85022	117.7176
1	11.9457	118.6596	11.88594	118.07	11.82647	117.4833

The effect of increasing bed thickness on the reaction rate causes the reaction rate to decrease

4.8.3 Potential Distribution

Tables (4.23_4.24) give the effect of bed thickness on the potential distribution.

Table 4.23 Effect of Bed thickness on the potential distribution in (V), flow rate **300 L / h** and copperic sulfate concentrations **0.001 and 0.01M**

X / L	2 cm		3 cm		4 cm	
	0.001 M	0.01 M	0.001 M	0.01 M	0.001 M	0.01 M
0	0.0674187	0.68211236	0.15139599	1.53177728	0.26862359	2.71788516
0.1	0.06674213	0.67526734	0.14987402	1.51637897	0.26591839	2.69051571
0.2	0.0647135	0.65474291	0.14531167	1.47021995	0.25781125	2.60849246
0.3	0.06133438	0.62055504	0.1377143	1.39335405	0.24431486	2.47194284
0.4	0.05660636	0.57271966	0.12708726	1.28583496	0.22544187	2.28099401
0.5	0.05053103	0.51125269	0.11343588	1.14771632	0.20120489	2.0357728
0.6	0.04310997	0.43617004	0.09676549	0.97905166	0.17161653	1.73640576
0.7	0.03434476	0.34748759	0.0770814	0.77989439	0.13668934	1.38301915
0.8	0.02423697	0.24522121	0.05438893	0.55029788	0.09643586	0.97573893
0.9	0.0127882	0.12938674	0.02869336	0.29031537	0.05086859	0.51469075
1	0	0	0	0	0	0

Table 4.24 Effect of Bed thickness on the potential distribution in (V), flow rate **500 L / h** and copperic sulfate concentrations **0.001 and 0.01M**

X / L	2 cm		3 cm		4 cm	
	0.001 M	0.01 M	0.001 M	0.01 M	0.001 M	0.01 M
0	0.0959632	0.97090913	0.21555729	2.1809287	0.38257473	3.87079259
0.1	0.09500068	0.96117101	0.21339198	2.15902155	0.37872593	3.83185301
0.2	0.0921144	0.93196955	0.20690039	2.09334373	0.36718982	3.71513765
0.3	0.08730629	0.88332416	0.19608902	1.98396059	0.34798181	3.52080131
0.4	0.08057829	0.81525419	0.18096437	1.83093742	0.32111727	3.24899851
0.5	0.07193231	0.72777898	0.16153292	1.63433936	0.28661153	2.89988346
0.6	0.06137027	0.62091785	0.13780115	1.3942315	0.24447993	2.47361004
0.7	0.04889411	0.49469011	0.10977552	1.1106788	0.19473774	1.97033186
0.8	0.03450573	0.34911505	0.07746249	0.78374615	0.13740021	1.39020219
0.9	0.01820706	0.18421193	0.04086851	0.41349832	0.07248257	0.73337401
1	0	0	0	0	0	0

The effect of increasing bed thickness on cathode potential is an increase behavior.

4.8.4 Solution Current Density Distribution

Tables (4.25_4.26) give the effect of bed thickness on the solution current density distribution.

Table 4.25 Effect of Bed thickness on the solution current density distribution in (A/m^2), flow rate 300 L / h and copperic sulfate concentrations 0.001 and 0.01M

X / L	2 cm		3 cm		4 cm	
	0.001 M	0.01 M	0.001 M	0.01 M	0.001 M	0.01 M
0	0	0	0	0	0	0
0.1	15.02953	149.2827	22.53768	223.8587	30.04142	298.3912
0.2	30.04142	298.3912	45.03567	447.3257	60.01231	596.0866
0.3	45.03567	447.3257	67.49404	670.4019	89.91285	893.0878
0.4	60.01231	596.0866	89.91285	893.0878	119.7432	1189.397
0.5	74.97137	744.6739	112.2922	1115.384	149.5035	1485.014
0.6	89.91285	893.0878	134.6321	1337.292	179.194	1779.943
0.7	104.8368	1041.329	156.9327	1558.811	208.8147	2074.184
0.8	119.7432	1189.397	179.194	1779.943	238.3659	2367.738
0.9	134.6321	1337.292	201.4161	2000.688	267.8478	2660.609
1	149.5035	1485.014	223.599	2221.047	297.2604	2952.796

Table 4.26 Effect of Bed thickness on the solution current density distribution in (A/m^2) flow rate 500 L / h and cupric sulfate concentrations 0.001 and 0.01M

X / L	2 cm		3 cm		4 cm	
	0.001 M	0.01 M	0.001 M	0.01 M	0.001 M	0.01 M
0	0	0	0	0	0	0
0.1	21.3825	212.3842	32.06571	318.4969	42.74357	424.5568
0.2	42.74357	424.5568	64.08322	636.5182	85.40148	848.2685
0.3	64.08322	636.5182	96.05259	954.0646	127.9739	1271.137
0.4	85.40148	848.2685	127.9739	1271.137	170.461	1693.163
0.5	106.6984	1059.808	159.8472	1587.735	212.8629	2114.35
0.6	127.9739	1271.137	191.6726	1903.861	255.1799	2534.698
0.7	149.2281	1482.255	223.4502	2219.515	297.4121	2954.209
0.8	170.461	1693.163	255.1799	2534.698	339.5596	3372.885
0.9	191.6726	1903.861	286.862	2849.41	381.6227	3790.728
1	212.8629	2114.35	318.4964	3163.651	423.6015	4207.739

Increasing bed thickness on the solution current density lead to increase the solution current density significantly.

Chapter Five

Discussion

In this chapter the figures, and their discussions, that describe the behavior of the simulation parameters are presented. These simulation results are classified into sections where feed concentration, volumetric flow rate, and bed length changes are studied to understand the reactor response to their variations.

First before presenting simulation results some of the assumptions made are explained. The first assumption is that of the one-dimensional model because of negligible dispersion effects in flow-through electrode so that the assumption of one-dimensional flow will save unnecessary time and effort wasted in solving the governing equations of two-dimensional models encountered in flow-by electrodes. Also the reason behind modeling with a flow direction from upstream to the downstream is that the electrolyte is allowed to penetrate into the deep portions of the bed and more contact will take place rather than flow from top of reactor where gravity as well as the flow itself will accelerate the electrolyte inside the bed. This advantage is well apparent in experimental works. The assumption of constant mass transfer coefficient along the bed will lead to a noticeable error when comparisons with experimental works will be made. This assumption is widely used in such works as well as non-plug flow effects can cause the predicted values by simulation to deviate from experimental results [23, 25].

5.1 Effect of Flow Rate

The effect of flow rate is presented in the followings on the concentration distribution, reaction rate, potential distribution, and current density distribution.

5.1.1 Concentration Distribution

The concentration distribution is found from equation (3.21)

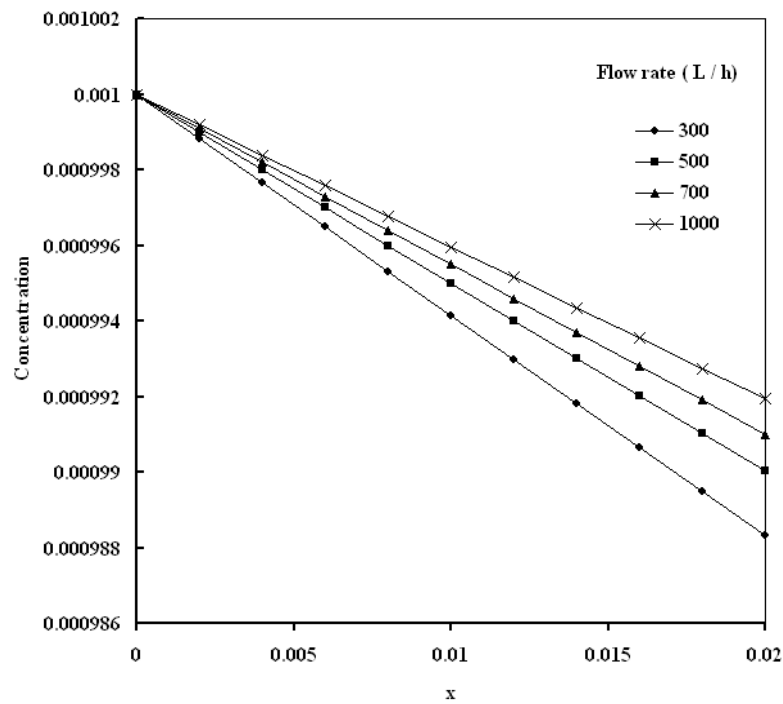


Fig. 5.1 Concentration distribution in 0.001M Cu^{2+} ion solution and 2cm bed thickness

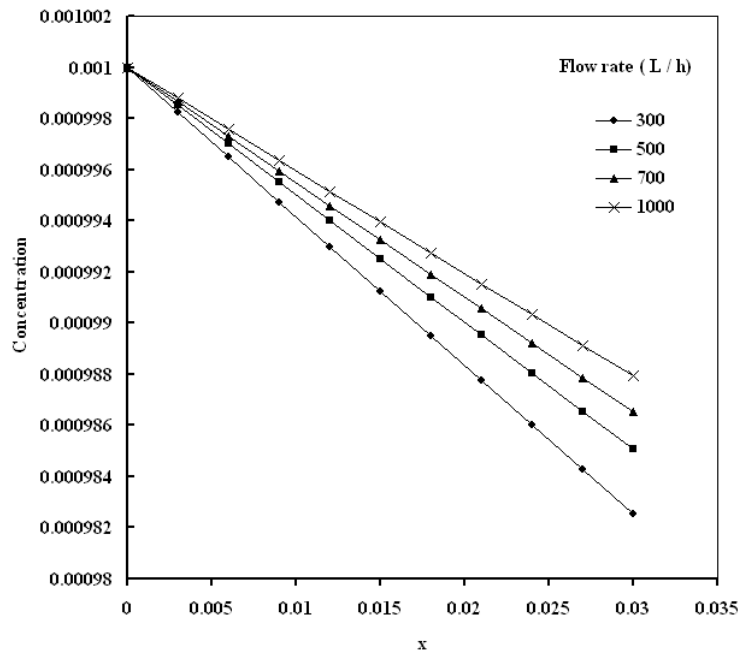


Fig. 5.2 Concentration distribution in 0.001M Cu^{2+} ion solution and 3cm bed thickness

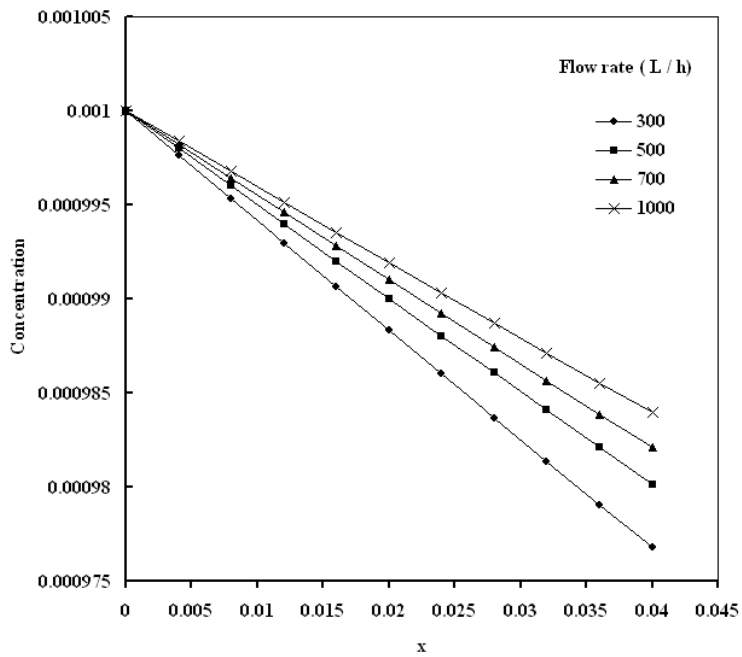


Fig. 5.3 Concentration distribution in 0.001M Cu^{2+} ion solution and 4cm bed thickness

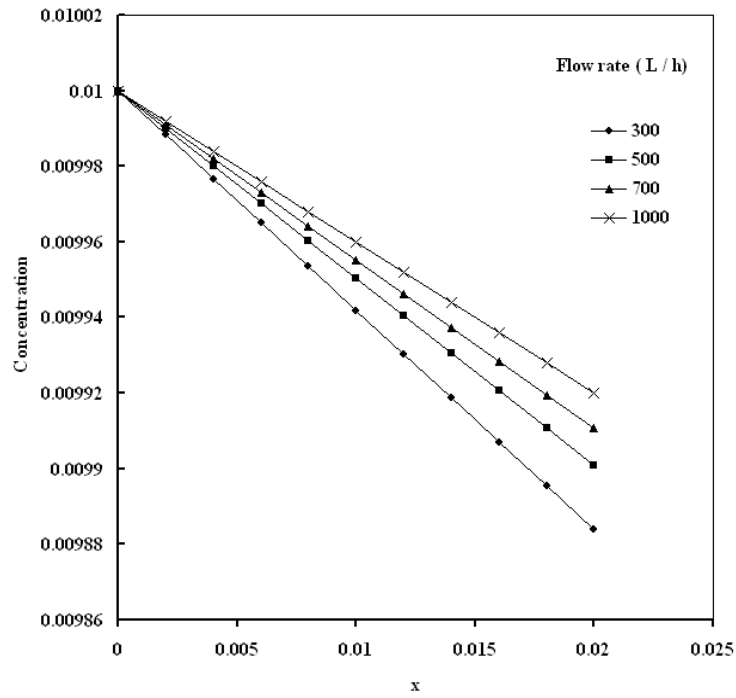


Fig. 5.4 Concentration distribution in 0.01M Cu^{2+} ion solution and 2cm bed thickness

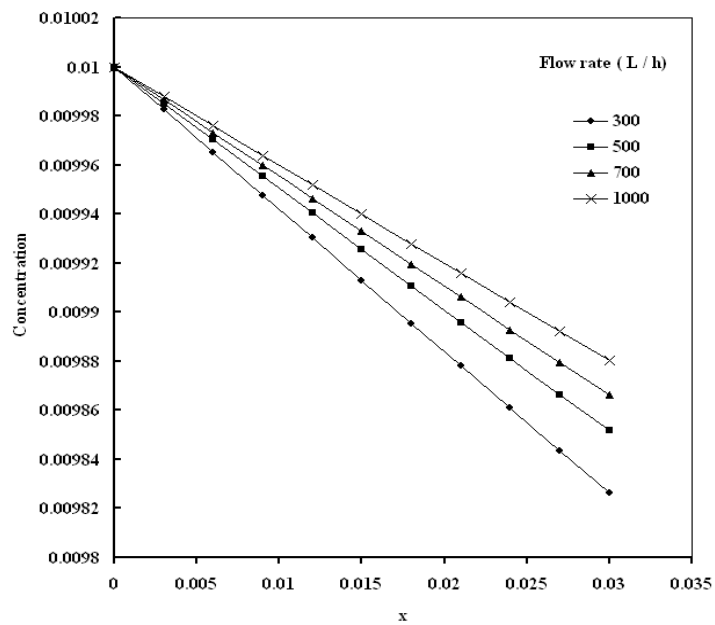


Fig. 5.5 Concentration distribution in 0.01M Cu^{2+} ion solution and 3cm bed thickness

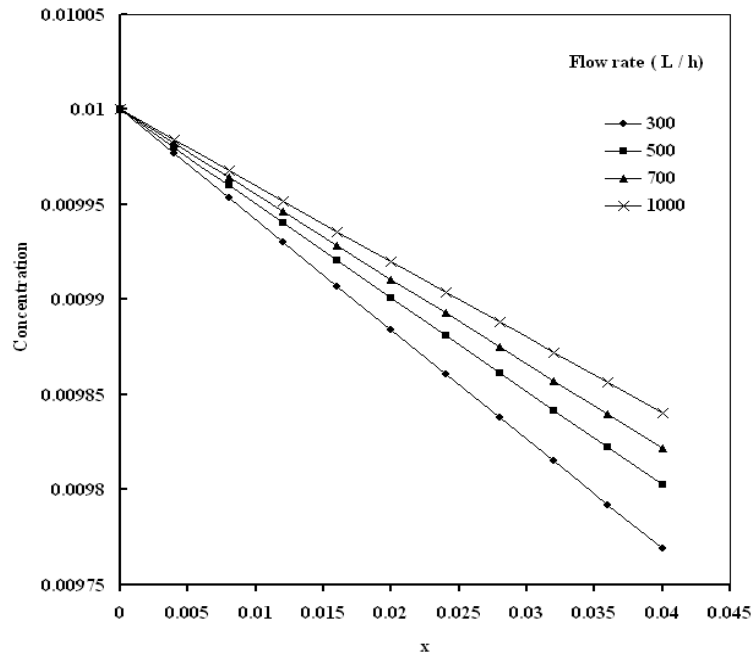


Fig. 5.6 Concentration distribution in 0.01M Cu^{2+} ion solution and 4cm bed thickness

Examining **Figs. 5.1-5.6** show that low concentration drop occurring when flow rate is increasing and vice versa. This due to the reason that at high flow rates the concentration drop within the packed bed is small under conditions of high flow rates, and large mass transfer coefficients as it was proved by Alkire and Gracon (1975) [23].

While for low flow rates the residence time of the copper ions will be greater than that of high flow rates therefore further conversion would be achieved.

5.1.2 Reaction Rate Distribution

The reaction rate distribution has been shown to be increase with flow rate equation (3.36). when flow rate is increased the reaction rates curves become so apart such it will be necessary to represent them individually as follows.

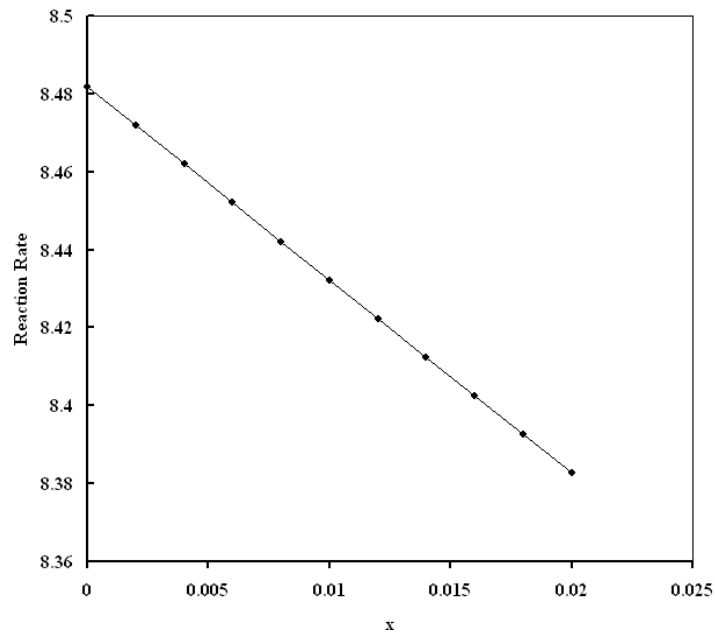


Fig. 5.7 Reaction rate distribution (A/m^2) in $0.001M$ Cu^{2+} ion solution, $2cm$ bed thickness, and flow rate $300 L / h$

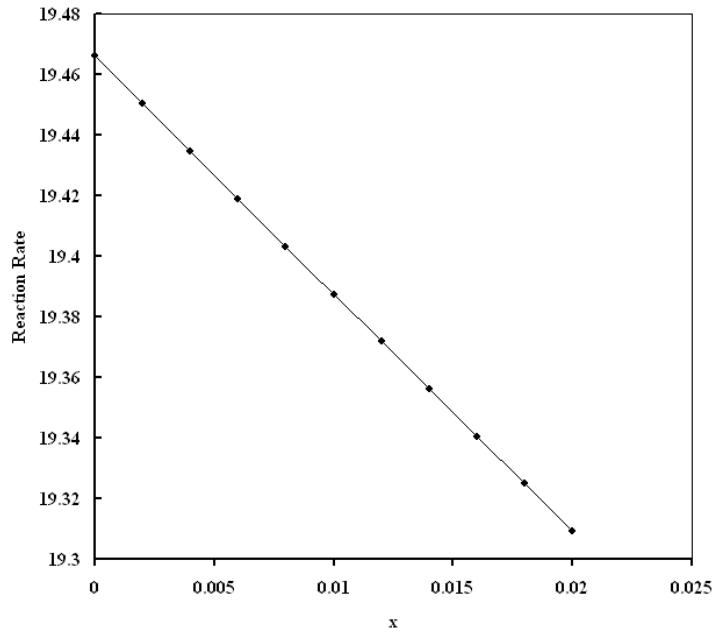


Fig. 5.8 Reaction rate distribution (A/m²) in 0.001M Cu²⁺ ion solution, 2cm bed thickness, and flow rate 1000 L / h

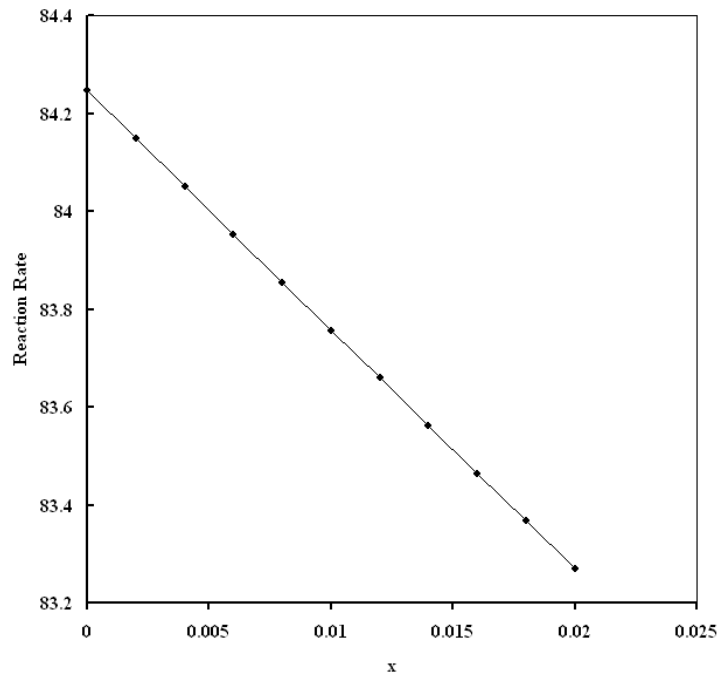


Fig. 5.9 Reaction rate distribution (A/m²) in 0.01M Cu²⁺ ion solution, 2cm bed thickness, and flow rate 300 L / h

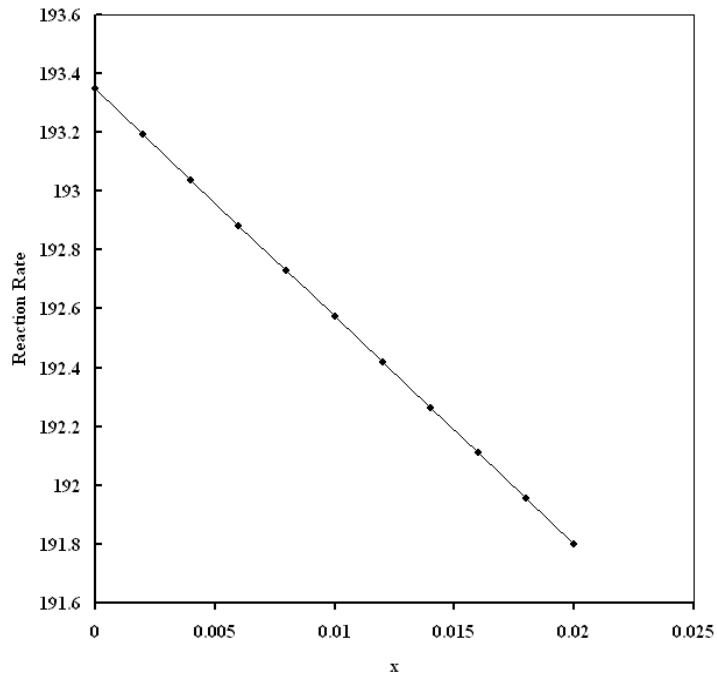


Fig. 5.10 Reaction rate distribution (A/m^2) in 0.001M Cu^{2+} ion solution, 2cm bed thickness, and flow rate 1000 L / h

Figures 5.7-5.10 demonstrates that the local limiting reaction rate (i_L) is decreasing with distance and this due to the consumption in the copperic sulfate ion which leads to decrease the reaction rate as for the effect of flow rate on reaction rate the reaction rate increases significantly with increasing flow rate this due to the increase in the mass transfer coefficient due to increased flow rate.

5.1.3 Potential Distribution

The potential distribution equation (3.34) is illustrated in the following figures.

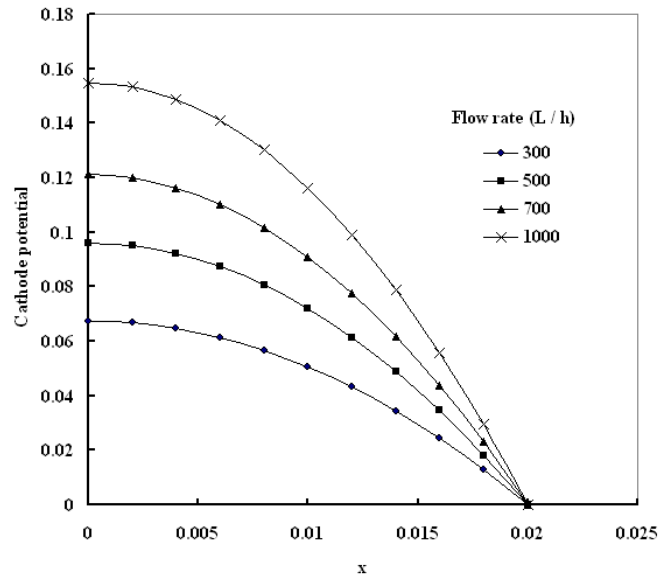


Fig. 5.11 Potential distribution (V) in 0.001M Cu^{2+} ion solution, 2cm bed thickness

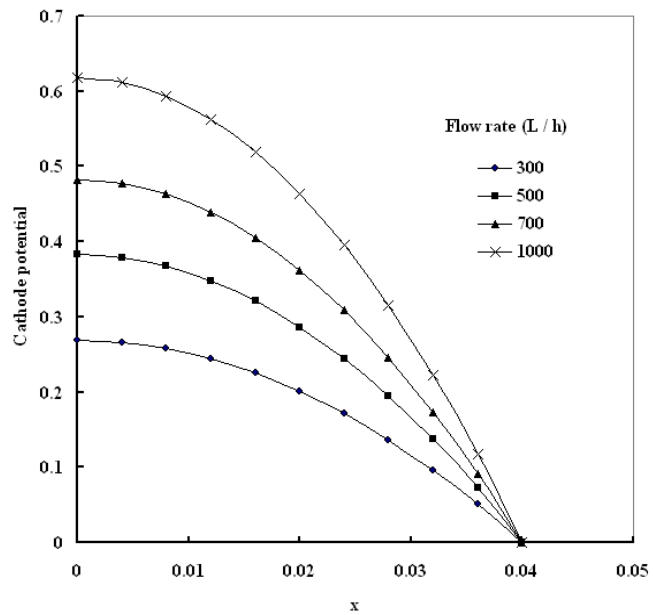


Fig. 5.12 Potential distribution (V) in 0.001M Cu^{2+} ion solution, 4cm bed thickness

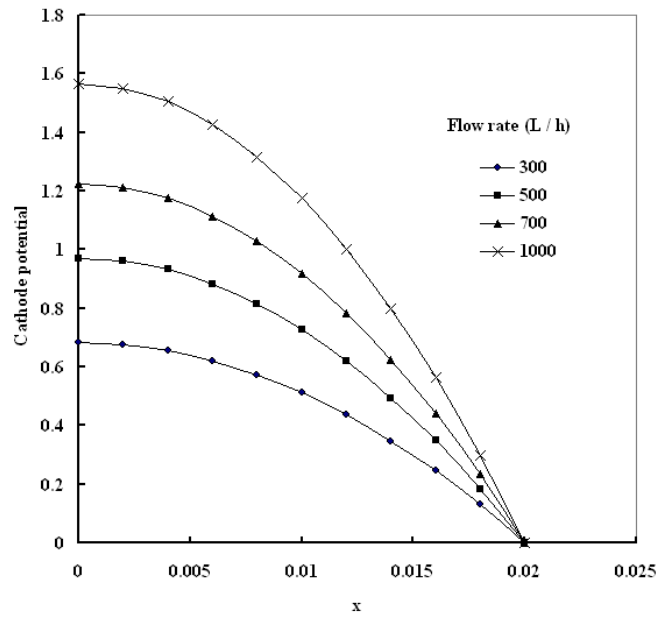


Fig. 5.13 Potential distribution (V) in 0.01M Cu^{2+} ion solution, 2cm bed thickness

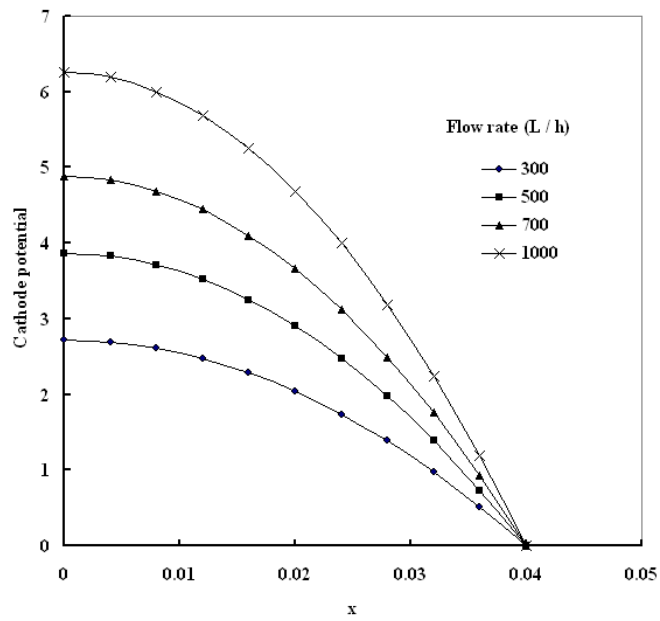


Fig. 5.14 Potential distribution (V) in 0.01M Cu^{2+} ion solution, 4cm bed thickness

The cathode potential is starting from a value close to the equilibrium value at the bed inlet (upstream) and deviate from the equilibrium as the electrolyte travels to the downstream which cause the reaction to take place, the cathode potential increases in value (absolute value) along the bed. The effect of increasing flow rate is to increase the cathode potential.

5.1.4 Solution Current Density Distribution

Which is given by equation (3.22)

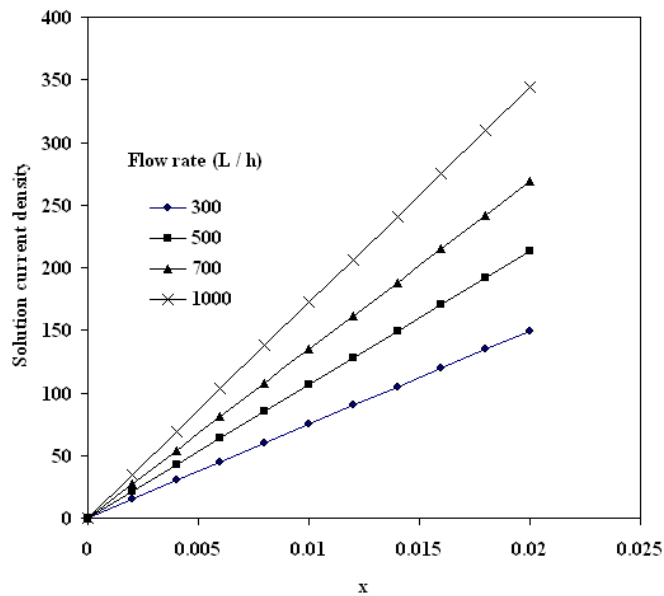


Fig. 5.15 Solution current density distribution (A/m^2) in $0.001M Cu^{2+}$ ion solution, 2cm bed thickness

The solution current density shown in **Fig. 5.15** is increasing with distance because as the electrolyte enters the bed all the current is within the metal phase and as the electrolyte proceeds the current will be transferred to the electrolyte until it reaches the maximum at the downstream where the current equals the total

current applied to the reactor (total limiting current density). The increase in the flow rate cause the solution current density to increase because of the increase in the total limiting current.

5.2 Effect of Cupric Sulfate Feed Concentration

5.2.1 Concentration Distribution

Table 5.1 Normalized concentration distribution for bed length 2 cm, flow rates 300, 500, 700, and 1000 L / h, and concentrations 0.001 and 0.01 M Cu^{2+} ion

Solution

x	300 L / h		500 L / h		700 L / h		1000 L / h	
	$C_b(x) / C_f$							
	0.001 M	0.01 M	0.001 M	0.01 M	0.001 M	0.01 M	0.001 M	0.01 M
0	1	1	1	1	1	1	1	1
0.002	0.99883	0.998833	0.999	0.999004	0.9991	0.999103	0.99919	0.999197
0.004	0.99765	0.997668	0.998	0.998009	0.99819	0.998206	0.99838	0.998394
0.006	0.99648	0.996504	0.997	0.997016	0.99729	0.997311	0.99758	0.997592
0.008	0.99531	0.995342	0.996	0.996023	0.99639	0.996416	0.99677	0.996791
0.01	0.99414	0.994181	0.995	0.995031	0.99549	0.995522	0.99596	0.99599
0.012	0.99297	0.993021	0.994	0.99404	0.99459	0.994629	0.99516	0.99519
0.014	0.99181	0.991863	0.993	0.99305	0.99369	0.993737	0.99435	0.99439
0.016	0.99064	0.990706	0.99201	0.992061	0.9928	0.992845	0.99355	0.993591
0.018	0.98948	0.98955	0.99101	0.991074	0.9919	0.991954	0.99274	0.992793
0.02	0.98832	0.988396	0.99002	0.990087	0.991	0.991064	0.99194	0.991996

Where the normalized concentration is $C_b(x) / C_f$

The effect of the concentration distribution presented in table 5.1 above for different flow rates shows that at low concentrations the cupric sulfate ion is

deposited faster but with finite difference from the 0.01 M concentration because of the low quantities of the cupric sulfate ions that will be consumed faster.

5.2.2 Reaction rate Distribution

Table 5.2 Reaction rate distribution in (A/m^2) for bed length 2 cm, flow rates 300 L / h, and Cu^{2+} ion solution concentrations 0.001 and 0.01 M

x	0.001 M	0.01 M
0	8.4818769	84.246923
0.002	8.4719153	84.148646
0.004	8.4619653	84.050482
0.006	8.4520271	83.952434
0.008	8.4421006	83.854499
0.01	8.4321857	83.756679
0.012	8.4222824	83.658973
0.014	8.4123908	83.561381
0.016	8.4025108	83.463903
0.018	8.3926424	83.366539
0.02	8.3827855	83.269288

Table 5.3 Reaction rate distribution in (A/m^2) for bed length 4 cm, flow rates 1000 L / h, and Cu^{2+} ion solution concentrations 0.001 and 0.01 M

0	19.466071	193.34831
0.004	19.434596	193.0378
0.008	19.403173	192.72778
0.012	19.3718	192.41826

0.016	19.340478	192.10924
0.02	19.309207	191.80071
0.024	19.277986	191.49268
0.028	19.246816	191.18514
0.032	19.215696	190.8781
0.036	19.184626	190.57155
0.04	19.153607	190.2655

Tables 5.2 and 5.3 show that the reaction rate is significantly increase with increasing feed concentration with a factor about 10 and this because of the increase in the quantity of the copperic sulfate ion that requires higher current to be treated.

5.2.3 Potential Distribution

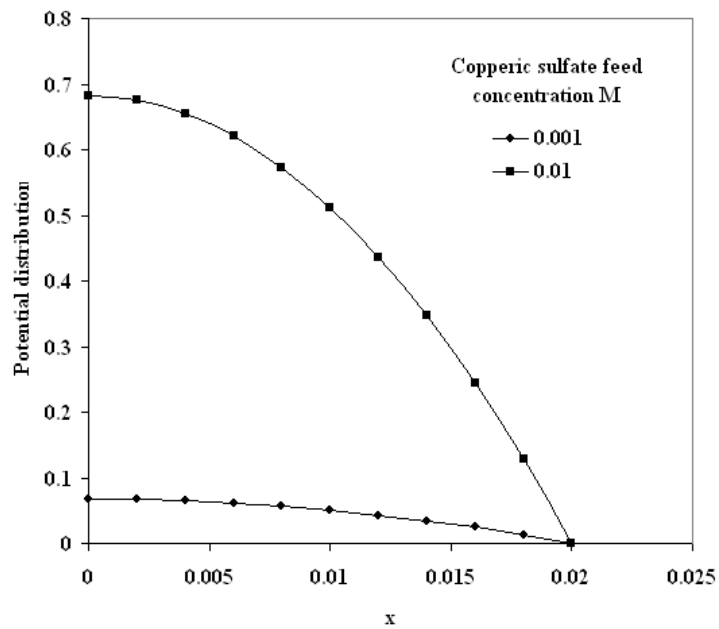


Fig. 5.16 Potential distribution (V) for flow rate 300 L / h, and bed thickness 2 cm

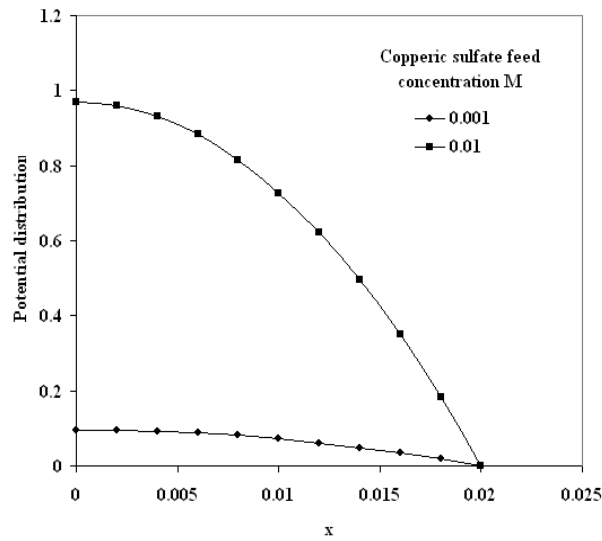


Fig. 5.17 Potential distribution (V) for flow rate 500 L / h, and bed thickness 2 cm

Figs. 5.16 and **5.17** show a significant increase in the potential distribution similar to that in the reaction rate and due to the same reason.

5.2.4 Solution Current Density Distribution

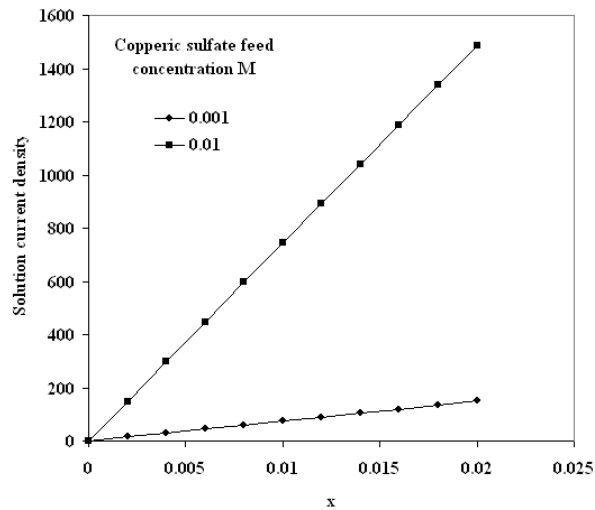


Fig. 5.18 Solution current density distribution in (A/m^2) for flow rate 300 L / h, and bed thickness 2 cm

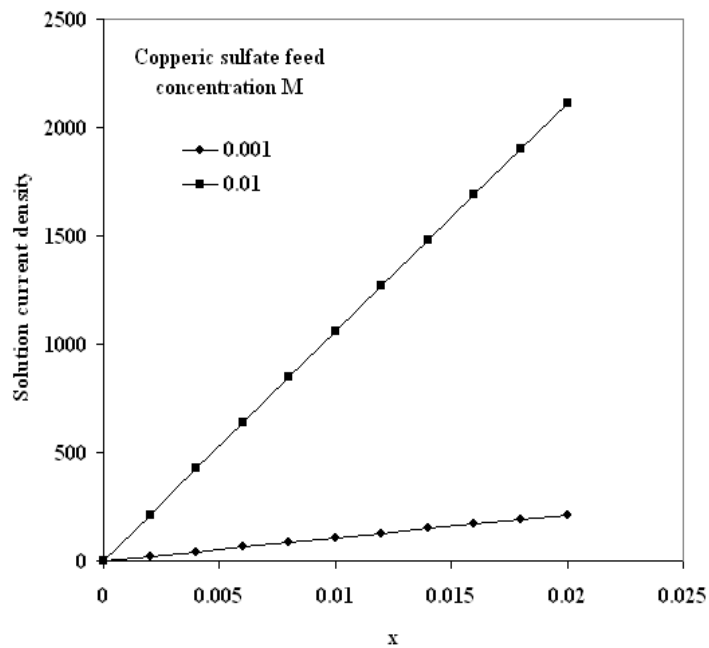


Fig. 5.19 Solution current density distribution in (A/m^2) for flow rate 500 L / h, and bed thickness 2 cm

Figs. 5.18 and **5.19** similar to the reaction rate, cathode potential show an increase in the solution current density due to the increase in the total current density.

5.3 Effect of Bed Thickness

5.3.1 Concentration Distribution

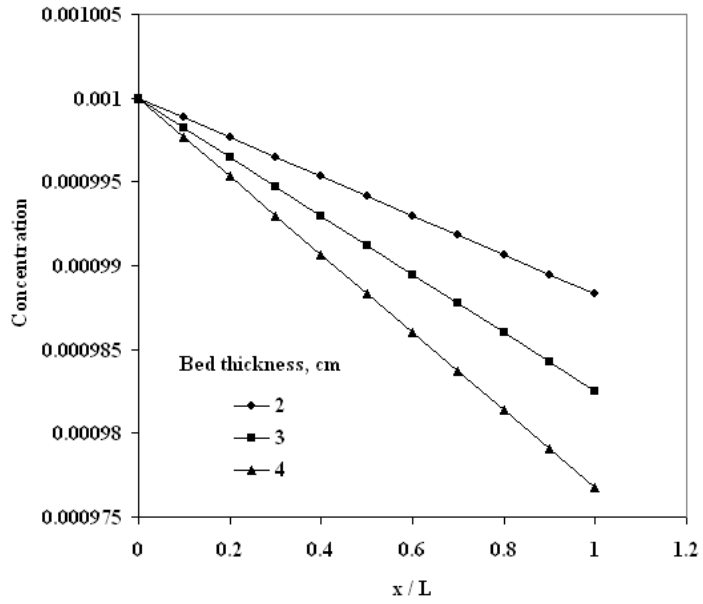


Fig. 5.20 Concentration distribution (M) in 0.001M Cu^{2+} ion solution, and flow rate 300 L/h

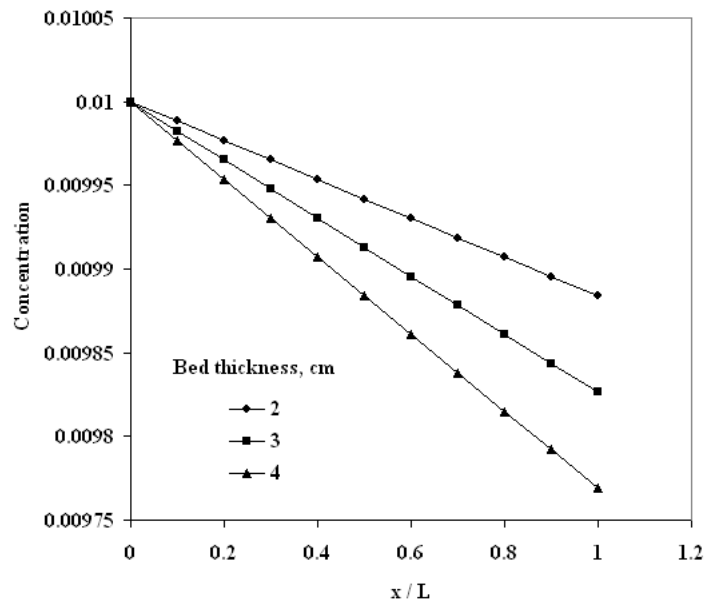


Fig. 5.21 Concentration distribution (M) in 0.01M Cu²⁺ ion solution, and flow rate 300 L / h

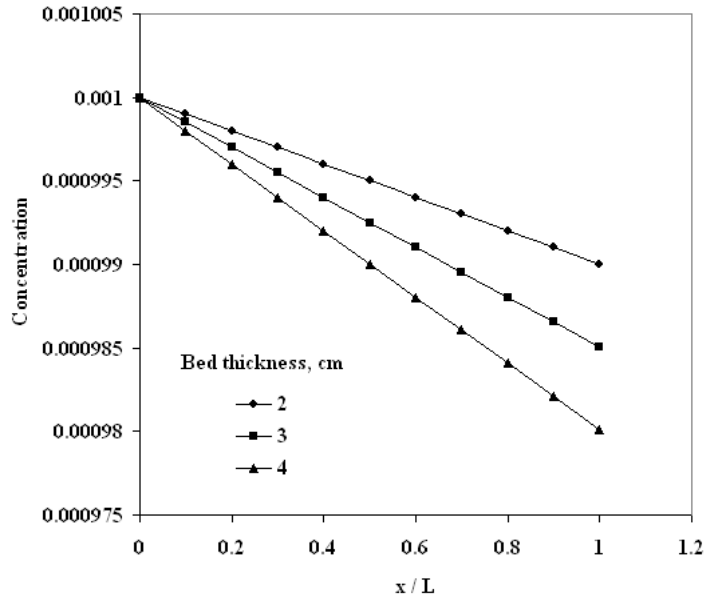


Fig. 5.22 Concentration distribution in 0.001M Cu²⁺ ion solution, and flow rate 500 L / h

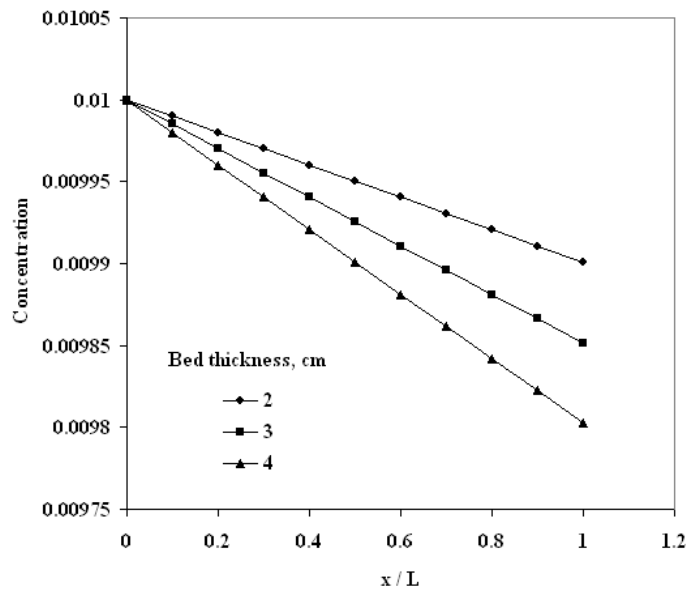


Fig. 5.23 Concentration distribution (M) in 0.01M Cu²⁺ ion solution, and flow rate 500 L / h

Examining the above figures show that the effect of increasing bed length causes the downstream concentration to decrease much more because more reaction is allowed to take place therefore decreasing the exit concentration of cupric sulfate.

5.3.2 Reaction Rate Distribution

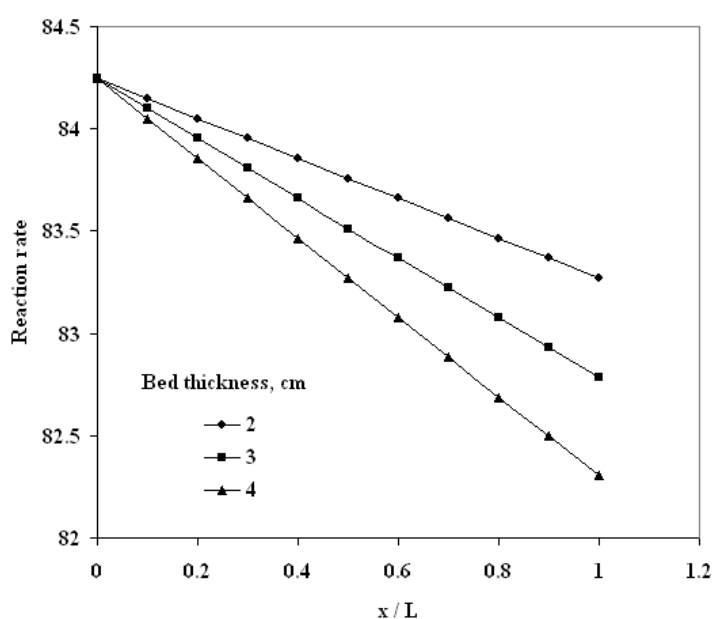


Fig. 5.24 Reaction rate distribution in (A/m²) in 0.001M Cu²⁺ ion solution, and flow rate 300 L / h

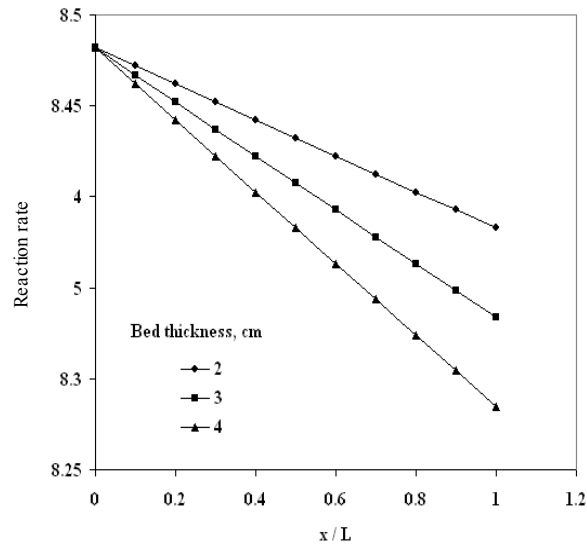


Fig. 5.25 Reaction rate distribution in (A/m^2) in $0.01M$ Cu^{2+} ion solution, and flow rate $300 L / h$

Figures 5.24 and 5.25 show that the reaction rate reaches lower values when bed thickness increases because of the consumption in the copper ions.

5.3.3 Potential Distribution

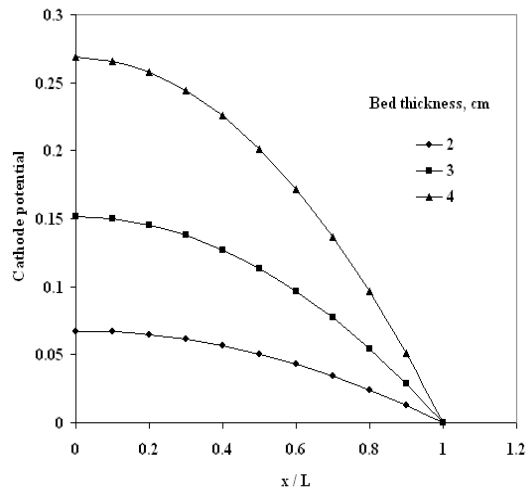


Fig. 5.26 Potential distribution (V) for flow rate $300 L / h$, and feed concentration of $0.001 M$

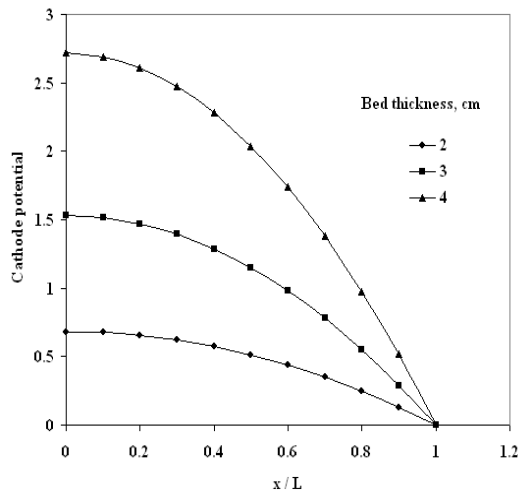


Fig. 5.27 Potential distribution (V) for flow rate 300 L / h, and feed concentration of 0.01 M

Figures 5.26 and 5.27 show that the cathode potential become greater when increasing bed thickness because of the more reaction that happened.

5.3.4 Solution Current Density Distribution

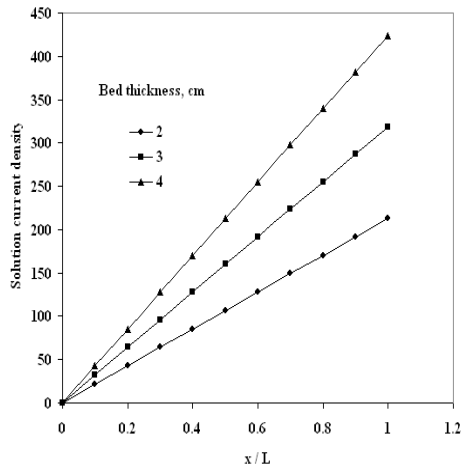


Fig. 5.28 Solution current density distribution in (A/m²) for flow rate 300 L / h, and feed concentration of 0.001 M

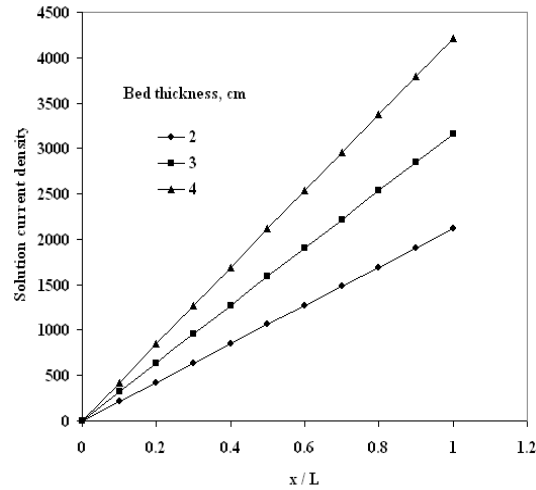


Fig. 5.29 Solution current density distribution in (A/m^2) for flow rate 300 L / h, and feed concentration of 0.01 M

Figures 5.28 and **5.29** demonstrate that the solution current density become greater when increasing bed thickness because of the increase in total limiting current density.

5.4 Comparison between Present Model and Literature

A comparison is made between present model and the experimental work of Olive and Lacoste (1979) [15] which is of similar configuration to present model, i.e. flow from bottom to the top of the reactor and mass transfer operation model, for the conditions $C_f = 0.009291$ M, $d_p = 0.00208$ m, Porosity = 0.4, $E(L) = 0.4$ V, and bed length of 1.5 cm.

Table 5.4 Cathode potential distribution (V) for the conditions of $C_f = 0.009291$ M, d_p 0.00208 m, Porosity = 0.4, $E(L) = 0.4$ V, and bed length of 1.5 cm given by Olive and Lacoste [15]

x	$u = 106 \times 10^{-4}$ m/s	$u = 44 \times 10^{-4}$ m/s	$u = 12 \times 10^{-4}$ m/s
0	0.144	0.253	0.341
0.002	0.150	0.253	0.347
0.003	0.155	0.258	0.353
0.004	0.164	0.261	0.355
0.005	0.170	0.267	0.356
0.006	0.182	0.282	0.358
0.007	0.194	0.283	0.359
0.008	0.205	0.288	0.361
0.009	0.220	0.305	0.367
0.01	0.238	0.311	0.370
0.011	0.252	0.323	0.373
0.012	0.270	0.329	0.376
0.013	0.285	0.341	0.382
0.014	0.317	0.352	0.388
0.015	0.338	0.364	0.391

The velocities given in table 5.4 above are converted to flow rates in Liters / h for packed bed diameter 4 cm

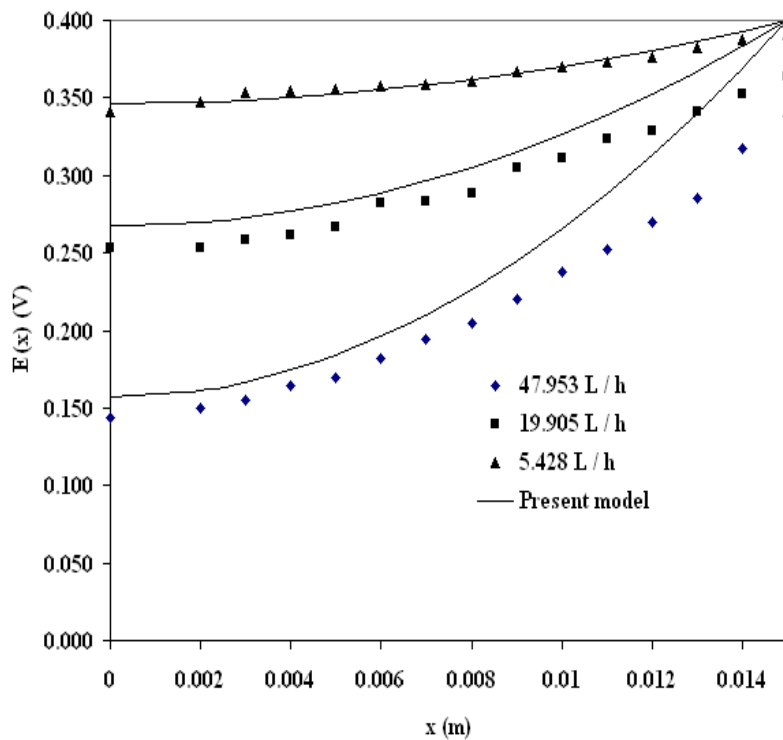


Fig. 5.30 Cathode potential distribution for the conditions of $C_f = 0.009291 \text{ M}$, $d_p = 0.00208 \text{ m}$, Porosity = 0.4, $E(L) = 0.4 \text{ V}$, and bed length of 1.5 cm given by Olive and Lacoste [15]

The comparison between present work and the experimental work [15] is indicating that the agreement is successful which leads to that the mathematical model is describing the behavior very well.

Chapter Six

Conclusions and Recommendations

6.1 Conclusions

Examining the present simulation results lead to the following conclusions:

1. The present model has successfully described the effect of flow rate, bed length, and feed concentration on the concentration distribution which has matched the expected from literature.
2. The electrodeposition rate is increasing when flow rate is increased due to the diffusion boundary layer near the cathode surface become thinner.
3. The electrodeposition rate is increasing when bed thickness is decreased.
4. The electrodeposition rate is increasing when feed concentration is increased this due to increasing mass transport to the cathode surface.
5. The model has been compared with the experimental work of Olive and Lacoste [15] under limiting current conditions, it gave a fairly good agreement.

6.2 Recommendations

1. The flow rates used in present work are relatively high flow rates and there is no experimental work available in the literature close enough to this work so that an experimental work with similar parameters to those studied is recommended for comparison purposes at different flow rates rather those studied in the work of Olive and Lacoste [15].
2. The present work did not study the effect of temperature therefore the study of the temperature as a variable is necessary in the future.
3. Studying another reactions may be may be proffered e.g. electro-organic reactions and side reactions such as hydrogen evolution may also be considered in the future.

References

1. Tobias, W.C.,” The coming of age of electrochemical engineering “, AIChE Symp. Ser., Vol. 77, No.204, 1981, pp2-9.
2. Walsh, F.C., “Electrochemical technology for environmental treatment and clean energy conversion”, Pure Appl. Chem., Vol.73, No.12, pp 1819-1837, 2001.
3. Kirk–Othmer, ”Encyclopedia of chemical technology”, 3rd edition, John Wiley and sons, 1981.
4. Fitzjohn, J. L., “Electro-organic synthesis” Chem. Eng. Prog. , Vol.71, No.2, 1972, pp. 85-87.
5. Clark, R. and Wasson, A., “Operational and treatment problems”, AIChE Symp. Ser., Vol. 79, No. 229, 1983, pp. 85-91.
6. Caldwell, D. L., “Overview of the industrial inorganic electrolytic process “, AIChE symp. Ser., Vol. 79, No.229, 1983.
7. Al-Shammari, A. A., Rahman, S.U., and Chin, D.T., ”An oblique rotating barrel electrochemical reactor for removal of copper ions from wastewater “J. Applied electrochem., Vol. 34, 2004.
8. Perry, R .H., Green, D. W., and Maloney, J. O. ” Perrey’s Chemical Engineers Handbook ”, 6th edition McGraw-Hill, 1984.
9. Pickett, David J., “ Electrochemical Reactor Design”, 2nd edition, Elsevier scientific publishing company, 1972.
- 10.Uhlig, H.H. and Revie, R. W., “ Corrosion and Corrosion Control”, John Wiley & Sons, 1985.
- 11.King, C. J., “Comments on the design of electrochemical cells”, AIChE Symp. Ser., Vol. 77, No. 204, 1981, pp. 46-58.

12. Bard, A. J. and Faulkner, L. R., "Electrochemical Methods fundamentals and application", John Wiley & Sons, 1980.
13. Wang, J. "Analytical electrochemistry", 2nd edition, John Wiley & Sons, 2001.
14. Risch, T. and Newman, J., "A theoretical comparison of flow-through and flow-by porous electrode at the limiting current", J. Electrochem. Soci, Vol.131, No.11, 1984.
15. Olive, H. and Lacoste, G." Application of Volumetric Electrodes To The Recuperation of Metals in Industrial Effluents –II Design of An Axial Field Flow-Through Porous Electrode", Electrochemi. Acta, Vol. 25, 1980, pp. 1303-1308.
16. Newman, J. and Tiedemann, W., "Porous electrode theory with battery applications", AIChE J., Vol. 21, No.1, 1975.
17. Kuhn, A. T. and Houghton, R.W., "A comparison of the performance of electrochemical reactor design in the treatment of dilute solutions", Electrochimica Acta, Vol. 19, 1974.
18. Masily, A.I. and Poddubny, N.P., "Influence of solid phase conductivity on spatial localization of electrochemical processes in flow through porous electrodes. Part II: Nonuniform porous matrix with variable conductivity profile", J. Applied electrochem, Vol.27, 1997.
19. Masily, A.I. and Poddubny, N.P., "Influence of solid phase conductivity on spatial localization of electrochemical processes in flow through porous electrodes. Part I: Electrodes with uniform conducting matrix", J. Applied electrochem. Vol.27, 1997.
20. Bertazzoli, R., Winder R. C., Marcos R. V. Lanza, Rozana A. Di Iglia, and Maria F.B. Sousa," Electrolytic removal of metals using a flow-through

- cell with a reticulated vitreous carbon cathode “, J. Braz. Chem. Soc. Vol. 8, No. 5, 1997.
21. Newman, J. and Tobias, C. W., ”Theoretical Analysis of current distribution in porous electrodes”, J. Electrochem. Soci, Vol.109, No.12, 1962.
22. Sioda, R. E., ”distribution of potential in a porous electrode under conditions of flow electrolysis”, Electrochim. Acta, vol.16, pp.1569- 1576, 1971.
23. Alkire, R., and Gracon, B., “Flow through porous electrodes”, J. Electrochem. Soci., Vol.122, No.12, 1975.
24. Coeuret, F., Hutin, D. and Gaundad, A. “Study of the effectiveness of fixed flow-through electrodes”, J. Appl. Electrochem., Vol.6, 1976, pp.417-423.
25. Trainham J. A. and Newman, J., ”A flow through porous electrode model: application to ion-removal from dilute streams “, J. Electrochem. Soci, Vol.124, No.10, 1977.
26. Gaundad, A., Hutin, D., and Coeuret, F., “Potential distribution in flow-through porous electrode under limiting current conditions”, Electrochemical Acta, Vol. 23, 1978.
27. Lahurd, D. A., ”Simplified models for use in electrochemical reactor Scale-up and system studies ”, J. Electrochem. Soci, Vol.132, No.12, 1985.
28. Al-Habobi, N. A. and Slaiman, Q. J., “Mass transfer measurements in electrochemical packed bed reactors for the reduction of Ti^{+4}/Ti^{+3} or Fe^{+3}/Fe^{+2} ”, Ph.D. Thesis, Saddam University, 2000.

29. Abdul-Masih, K. S., Sulaymon, A. H., Slaiman, Q. J., and Majeed, M., "Design of flow-through porous electrochemical reactor working under limiting current conditions", Ph.D. Thesis, Baghdad University, 2001.
30. Hunson, M., Vergnes, H., Pruksathorn, P., Damronglerd, S., "Recovering of copper from synthetic solution in 3PE reactor", Science Asia No. 28, 2002.
31. Ruotolo, L.M., and Gubulin, J. C., "Electrodeposition of copper ions on fixed bed electrodes: kinetic and hydrodynamic study", Brazilian journal of chemical engineering, Vol. 19, No. 1, 2002.
32. Jolls, K.R. and Hanratty, T.J., A.I.Ch.E. Journal, Vol.15, 1969.
33. Yip, H.H-K, "Mass transfer coefficient in packed beds at low Reynolds numbers", M.Sc. Thesis, University of California, 1973.
34. Wilson, E.J., and Geankopolis C.J., Ind. Eng. Chem. Fund., Vol.5, 1966.
35. Oloman, C. and Reilly, P., "Modeling and parameter estimation for a fixed bed electrochemical reactor", J. Electrochem. Soc., Vol. 134, No. 4, 1987.
36. Furnas, C.C., Ind. Eng. Chem., Vol. 23, 1993, p. 1052.
37. Horvath, A.L., "Handbook Aqueous of Electrolyte Solutions", Ellis Horwood Limited, 1985.
38. Savinell, R. F., "Some aspects of electrochemical reactor design", AIChE Symp. Ser. Vol. 79, No. 229, 1983, pp. 13-24.
39. Newman, J., "Simultaneous reactions at disk and porous electrodes", Electrochimica Acta, Vol. 22, 1977, pp. 903-911.
40. Selman, J. R., "Dimensional analysis and scale-up of electrochemical reactors", AIChE Symp. Ser., Vol. 79, No. 229, 1983, pp. 101-110.
41. Neale, G. H. and Nader, W.K., A.I.Ch.E. Journal, Vol. 19, 1973.

42. Munji, S.T., AbdulMasih, K.S., Slaiman, Q.J., "Simple model electrochemical Reactor for simulation studies", Msc. Thesis, Nahrain University, 2006.

Appendix A

Tables of Results

Table A.1 Effect of flow rate on the concentration distribution in M for bed thickness of 2 cm, feed concentration 0.01 M

x (m)	300 L / h	500 L / h	700 L / h	1000 L / h
0.000	0.01	0.01	0.01	0.01
0.002	0.00998833	0.00999004	0.00999103	0.00999197
0.004	0.00997668	0.00998009	0.00998206	0.00998394
0.006	0.00996504	0.00997016	0.00997311	0.00997592
0.008	0.00995342	0.00996023	0.00996416	0.00996791
0.010	0.00994181	0.00995031	0.00995522	0.0099599
0.012	0.00993021	0.0099404	0.00994629	0.0099519
0.014	0.00991863	0.0099305	0.00993737	0.0099439
0.016	0.00990706	0.00992061	0.00992845	0.00993591
0.018	0.0098955	0.00991074	0.00991954	0.00992793
0.020	0.00988396	0.00990087	0.00991064	0.00991996

Table A.2 Effect of flow rate on the concentration distribution in M for bed thickness of 3 cm, feed concentration 0.01 M

x (m)	300 L / h	500 L / h	700 L / h	1000 L / h
0.000	0.01	0.01	0.01	0.01
0.003	0.00998251	0.00998507	0.00998655	0.00998795
0.006	0.00996504	0.00997016	0.00997311	0.00997592
0.009	0.00994761	0.00995527	0.00995969	0.0099639
0.012	0.00993021	0.0099404	0.00994629	0.0099519
0.015	0.00991284	0.00992556	0.00993291	0.00993991
0.018	0.0098955	0.00991074	0.00991954	0.00992793
0.021	0.00987819	0.00989594	0.00990619	0.00991597
0.024	0.00986091	0.00988116	0.00989287	0.00990403
0.027	0.00984366	0.0098664	0.00987956	0.00989209
0.030	0.00982644	0.00985167	0.00986626	0.00988018

Table A.3 Effect of flow rate on the concentration distribution in M for bed thickness of 4 cm, feed concentration 0.01 M

x (m)	300 L / h	500 L / h	700 L / h	1000 L / h
0.000	0.01	0.01	0.01	0.01
0.004	0.00997668	0.00998009	0.00998206	0.00998394
0.008	0.00995342	0.00996023	0.00996416	0.00996791
0.012	0.00993021	0.0099404	0.00994629	0.0099519
0.016	0.00990706	0.00992061	0.00992845	0.00993591
0.020	0.00988396	0.00990087	0.00991064	0.00991996
0.024	0.00986091	0.00988116	0.00989287	0.00990403
0.028	0.00983792	0.00986149	0.00987512	0.00988812
0.032	0.00981498	0.00984186	0.00985741	0.00987224
0.036	0.00979209	0.00982227	0.00983973	0.00985639
0.040	0.00976926	0.00980272	0.00982208	0.00984056

Table A.4 Effect of flow rate on the reaction rate distribution in (A/m^2) for bed thickness of 2 cm, feed concentration 0.01 M

x (m)	300 L / h	500 L / h	700 L / h	1000 L / h
0.000	84.246923	119.8477	151.16736	193.34831
0.002	84.148646	119.72835	151.03173	193.19299
0.004	84.050482	119.60913	150.89623	193.0378
0.006	83.952434	119.49002	150.76085	192.88272
0.008	83.854499	119.37104	150.62558	192.72778
0.010	83.756679	119.25217	150.49044	192.57296
0.012	83.658973	119.13342	150.35542	192.41826
0.014	83.561381	119.01479	150.22053	192.26369
0.016	83.463903	118.89628	150.08575	192.10924
0.018	83.366539	118.77788	149.95109	191.95491
0.020	83.269288	118.6596	149.81656	191.80071

Table A.5 Effect of flow rate on the reaction rate distribution in (A/m^2) for bed thickness of 3 cm, feed concentration 0.01 M

x (m)	300 L / h	500 L / h	700 L / h	1000 L / h
0.000	84.246923	119.8477	151.16736	193.34831
0.003	84.09955	119.66873	150.96397	193.11538
0.006	83.952434	119.49002	150.76085	192.88272
0.009	83.805575	119.31159	150.558	192.65035
0.012	83.658973	119.13342	150.35542	192.41826
0.015	83.512628	118.95552	150.15312	192.18645
0.018	83.366539	118.77788	149.95109	191.95491
0.021	83.220705	118.60051	149.74933	191.72366
0.024	83.075126	118.4234	149.54785	191.49268
0.027	82.929802	118.24656	149.34663	191.26198
0.030	82.784733	118.06998	149.14569	191.03156

Table A.6 Effect of flow rate on the concentration distribution in (A/m^2) for bed thickness of 4 cm, feed concentration 0.01 M

x (m)	300 L / h	500 L / h	700 L / h	1000 L / h
0.000	84.246923	119.8477	151.16736	193.34831
0.004	84.050482	119.60913	150.89623	193.0378
0.008	83.854499	119.37104	150.62558	192.72778
0.012	83.658973	119.13342	150.35542	192.41826
0.016	83.463903	118.89628	150.08575	192.10924
0.020	83.269288	118.6596	149.81656	191.80071
0.024	83.075126	118.4234	149.54785	191.49268
0.028	82.881418	118.18767	149.27962	191.18514
0.032	82.688161	117.95241	149.01187	190.8781
0.036	82.495354	117.71762	148.74461	190.57155
0.040	82.302997	117.48329	148.47782	190.2655

Table A.7 Effect of flow rate on the potential distribution in (V) for bed thickness of 2 cm, feed concentration 0.01 M

x (m)	300 L / h	500 L / h	700 L / h	1000 L / h
0.000	0.682112361	0.970909132	1.225037997	1.567356298
0.002	0.675267336	0.961171005	1.212754612	1.551644929
0.004	0.654742908	0.931969554	1.175919152	1.504527653
0.006	0.620555035	0.883324161	1.114553646	1.426029699
0.008	0.572719656	0.815254187	1.028680101	1.316176275
0.010	0.511252691	0.727778976	0.918320506	1.174992569
0.012	0.436170043	0.62091785	0.78349683	1.00250375
0.014	0.347487594	0.494690114	0.624231022	0.798734966
0.016	0.245221209	0.349115053	0.440545011	0.563711345
0.018	0.129386735	0.184211933	0.232460707	0.297457993
0.020	0	0	0	0

Table A.8 Effect of flow rate on the potential distribution in (V)for bed thickness of 3 cm, feed concentration 0.01 M

x (m)	300 L / h	500 L / h	700 L / h	1000 L / h
0.000	1.531777281	2.180928698	2.752222797	3.521839249
0.003	1.516378969	2.159021549	2.724589314	3.486493404
0.006	1.470219955	2.093343727	2.641738446	3.38051265
0.009	1.393354047	1.983960594	2.503744486	3.203982084
0.012	1.285834963	1.830937416	2.31068163	2.956986701
0.015	1.147716322	1.63433936	2.062623971	2.639611391
0.018	0.979051655	1.394231499	1.759645507	2.251940944
0.021	0.779894395	1.110678804	1.401820131	1.794060048
0.024	0.550297883	0.783746152	0.98922164	1.266053286
0.027	0.290315366	0.413498323	0.52192373	0.668005143
0.030	0	0	0	0

Table A.9 Effect of flow rate on the potential distribution in (V)for bed thickness of 4 cm, feed concentration 0.01 M

x (m)	300 L / h	500 L / h	700 L / h	1000 L / h
0.000	2.717885163	3.87079259	4.885545434	6.25268671
0.004	2.69051571	3.831853012	4.836426589	6.189858065
0.008	2.608492457	3.715137645	4.689187538	6.001506686
0.012	2.471942844	3.520801308	4.444004267	5.687834162
0.016	2.280994011	3.248998511	4.101052448	5.249041756
0.020	2.035772801	2.899883458	3.660507437	4.685330412
0.024	1.736405765	2.473610044	3.122544277	3.996900747
0.028	1.383019154	1.97033186	2.487337695	3.183953059
0.032	0.975738928	1.390202189	1.755062105	2.246687323
0.036	0.514690753	0.733374011	0.925891611	1.185303192
0.040	0	0	0	0

Table A.10 Effect of cupric sulfate concentration on the concentration distribution in (M) for bed thickness of 3 cm, and flow rates 300 and 500 L / h

x (m)	0.001 M		0.01 M	
	300 L / h	500 L / h	300 L / h	500 L / h
0.000	0.001	0.001	0.01	0.01
0.004	0.00099765	0.000998	0.00997668	0.00998009
0.008	0.00099531	0.000996	0.00995342	0.00996023
0.012	0.00099297	0.000994	0.00993021	0.0099404
0.016	0.00099064	0.00099201	0.00990706	0.00992061
0.020	0.00098832	0.00099002	0.00988396	0.00990087
0.024	0.000986	0.00098804	0.00986091	0.00988116
0.028	0.00098368	0.00098606	0.00983792	0.00986149
0.032	0.00098137	0.00098408	0.00981498	0.00984186
0.036	0.00097907	0.00098211	0.00979209	0.00982227
0.040	0.00097677	0.00098014	0.00976926	0.00980272

Table A.11 Effect of cupric sulfate concentration on the concentration distribution in (M) for bed thickness of 3 cm, and flow rates 700 and 1000 L / h

x (m)	0.001 M		0.01 M	
	700 L / h	1000 L / h	700 L / h	1000 L / h
0.000	0.001	0.001	0.01	0.01
0.004	0.00099819	0.00099838	0.00998206	0.00998394
0.008	0.00099639	0.00099677	0.00996416	0.00996791
0.012	0.00099459	0.00099516	0.00994629	0.0099519
0.016	0.0009928	0.00099355	0.00992845	0.00993591
0.020	0.000991	0.00099194	0.00991064	0.00991996
0.024	0.00098921	0.00099034	0.00989287	0.00990403
0.028	0.00098743	0.00098874	0.00987512	0.00988812
0.032	0.00098564	0.00098714	0.00985741	0.00987224
0.036	0.00098387	0.00098554	0.00983973	0.00985639
0.040	0.00098209	0.00098395	0.00982208	0.00984056

Appendix B

Sample of Calculations

Conditions:

1. Electrolyte concentration 0.001 M CuSO₄ and 0.5 M H₂SO₄
 2. flow rate 300 L / h
 3. Particle diameter 4 mm
 4. Bed thickness 2 cm and diameter 4 cm
- A. Evaluation of physical properties:-

Density calculation form chemical engineers handbook (Perry) [8]

$$\rho = 1023 \text{ kg / m}^3$$

And from previous work [42]

$$\rho = 1103.262 + 61.46M_{H_2SO_4} + 131M_{CuSO_4} + 77.63(M_{H_2SO_4} \cdot M_{CuSO_4})^{0.0232} - 180M_{CuSO_4}^{0.0086M_{H_2SO_4}} \quad \dots(B.1)$$

$$\rho = 1103.262 + 61.46 * 0.5 + 131 * 0.001 + 77.63(0.5 * 0.001)^{0.0232} - 180 * 0.001^{0.0086 * 0.5} = 1024.47 \text{ kg / m}^3$$

Viscosity calculation form chemical engineers handbook (Perry) [8]

$$\mu = 1.15 * 10^{-3} \text{ kg / m s}$$

And from previous work [42]

$$\mu = -3 \times 10^{-3} + 2.23 \times 10^{-4} M_{H_2SO_4} + 8.3 \times 10^{-7} M_{CuSO_4} - 8.3 \times 10^{-7} (M_{H_2SO_4} \cdot M_{CuSO_4})^{0.14} + 0.00406 M_{CuSO_4}^{2.287 \times 10^{-3} M_{H_2SO_4}} \quad \dots(B.2)$$

$$\mu = -3 \times 10^{-3} + 2.23 \times 10^{-4} * 0.5 + 8.3 \times 10^{-7} * 0.001 - 8.3 \times 10^{-7} (0.5 * 0.001)^{0.14} + 0.00406 * 0.001^{2.287 \times 10^{-3} * 0.5} = 1.1393 * 10^{-3} \text{ kg / m s}$$

Calculation of electrical conductivity in the bulk electrolyte

$$\begin{aligned} \kappa_o &= 74.92 - 6.1459M_{CuSO_4} - 25.7M_{H_2SO_4} - \\ & 3.92M_{CuSO_4}M_{H_2SO_4}^{8.6} + 5.144M_{CuSO_4}^{-0.139M_{H_2SO_4}} \quad \dots(B.3) \\ \kappa_o &= 74.92 - 6.1459 * 0.001 - 25.7 * 0.5 - \\ & 3.92 * 0.001 * 0.5^{8.6} + 5.144 * 0.001^{-0.139 * 0.5} = 70.377 \Omega^{-1} m^{-1} \end{aligned}$$

Calculation of diffusion coefficient from Stokes-Einstein equation at 25°C

$$\begin{aligned} D &= \frac{3.36 * 10^{-12}}{\mu^{0.74}} \quad \dots(3.9) \\ D &= \frac{3.36 * 10^{-12}}{(1.1393 * 10^{-3})^{0.74}} = 5.063 * 10^{-12} m^2 / s \end{aligned}$$

The actual conductivity in bed κ is found by Neale [41] :-

$$\frac{\kappa}{\kappa_o} = \frac{2\varepsilon}{(3 - \varepsilon)} \quad \dots(B.4)$$

B. Evaluation of bed parameters

Bed porosity by Furnas [36]

$$\varepsilon = 0.375 + 0.34 \frac{d}{D_R} \quad \dots(3.7)$$

$$\varepsilon = 0.375 + 0.34 \frac{0.004}{0.04} = 0.409$$

$$\kappa = 70.377671 \frac{2 * 0.409}{(3 - 0.409)} = 22.2188 \Omega^{-1} m^{-1}$$

$$\text{Flow rate in SI units} = \frac{300L}{h} \Big| \frac{m^3}{1000L} \Big| \frac{h}{3600s} = 8.333333 * 10^{-5} m^3 / s$$

$$\text{Cross-sectional area} = \frac{\pi}{4} D_R^2 = \frac{\pi}{4} 0.04^2 = 1.256637 * 10^{-3} m^2$$

$$\text{Specific surface area (a)} = \frac{6}{d} (1 - \varepsilon) = \frac{6}{d} (1 - 0.409) = 886.5 m^{-1}$$

$$\text{Electrolyte velocity (u)} = 8.333333 * 10^{-5} / 1.256637 * 10^{-3} = 0.066314 \text{ m/s}$$

C. Evaluation of concentration profile

$$C_b = C_f e^{mx} \quad \dots(3.21)$$

$$Re = \rho u d / \mu = (1024.477 * 0.066314 * .004) / 1.1393 * 10^{-3} = 238.52939$$

$$Sc = \mu / \rho D = 1.1393 * 10^{-3} / (1024.477 * 5.063^{-10}) = 2196.3$$

Calculation of the mass transfer coefficient (k) by Wilson and Geankoplis correlation [34]

$$\frac{k}{u} = \frac{0.25}{\varepsilon} Re^{-0.31} Sc^{-2/3} \quad \dots(3.6)$$

valid for $55 < Re < 1500$ and $165 < Sc < 10690$.

$$k = 0.0066314 \frac{0.25}{0.409} 238.52939^{-0.31} 2196.3^{-2/3} = 4.3953 * 10^{-5} m/s$$

$$m = \frac{0.066314 - \sqrt{0.066314^2 + 4 * 886.5 * 4.3953 * 10^{-4} * 5.063 * 10^{-10}}}{2 * 5.063 * 10^{-10}} = -0.5873$$

$$C_b = 0.001 e^{-0.5873x}$$

Substituting x values from zero to 0.02 m as follows:

x(m)	Cb	Value of Cb in M
0	0.001*exp(0)	0.001
0.002	0.001*exp(-0.5873*0.002)	0.000998826
0.004	0.001*exp(-0.5873*0.004)	0.00099765
0.006	0.001*exp(-0.5873*0.006)	0.00099531
0.008	0.001*exp(-0.5873*0.008)	0.00099414
0.01	0.001*exp(-0.5873*0.001)	0.00099297

0.012	0.001*exp(-0.5873*0.012)	0.00099181
0.014	0.001*exp(-0.5873*0.014)	0.0009906
0.016	0.001*exp(-0.5873*0.016)	0.00098894
0.018	0.001*exp(-0.5873*0.018)	0.00098832
0.02	0.001*exp(-0.5873*0.02)	0.000988322

D. Evaluation of potential distribution

$$E(x) - E(L) = \frac{uzFC_f}{m\kappa} [e^{mx} - e^{mL} + m(L-x)] \quad \dots(3.34)$$

Converting $C_f = 0.001 \text{ M (g mol / L)} = 1 \text{ g mol / m}^3$

$F = 96487 \text{ C / g mol equivalent}$

$$E(x) - E(L) = \frac{0.006314 * 2 * 96487 * 1}{-0.5873 * 22.2188} [e^{-0.5873x} - e^{-0.5873L} - 0.5873(0.02 - x)]$$

$$E(x) - E(L) = -980.68 [e^{-0.5873x} - e^{-0.5873L} - 0.5873(0.02 - x)]$$

x(m)	E(x) - E(L)	Value in V
0	-980.68[exp(0)-exp(0.5873*0.02)-0.5873(0.02-0)]	0.067387
0.002	-980.68[exp(-0.5873*0.002)-exp(0.5873*0.02)-0.5873(0.02-0.002)]	0.06671
0.004	-980.68[exp(-0.5873*0.004)-exp(0.5873*0.02)-0.5873(0.02-0.004)]	0.06468
0.006	-980.68[exp(-0.5873*0.006)-exp(0.5873*0.02)-0.5873(0.02-0.006)]	0.061305
0.008	-980.68[exp(-0.5873*0.008)-exp(0.5873*0.02)-0.5873(0.02-0.008)]	0.05658
0.01	-980.68[exp(-0.5873*0.01)-exp(0.5873*0.02)-0.5873(0.02-0.01)]	0.050507
0.012	-980.68[exp(-0.5873*0.012)-exp(0.5873*0.02)-0.5873(0.02-0.012)]	0.043089
0.014	-980.68[exp(-0.5873*0.014)-exp(0.5873*0.02)-0.5873(0.02-0.014)]	0.03432
0.016	-980.68[exp(-0.5873*0.016)-exp(0.5873*0.02)-0.5873(0.02-0.016)]	0.02422
0.018	-980.68[exp(-0.5873*0.018)-exp(0.5873*0.02)-0.5873(0.02-0.018)]	0.01278
0.02	-980.68[exp(-0.5873*0.02)-exp(0.5873*0.02)-0.5873(0.02-0.02)]	0

E. Evaluation of the reaction rate as a function of x

$$i_L(x) = zFkC_f e^{mx} \quad \dots(3.36)$$

$$i_L(x) = 2 * 96487 * 4.395 * 10^{-5} * 1 e^{-0.5873x}$$

$$i_L(x) = 8.4812073 e^{-0.5873x}$$

x(m)	i_L	Value in A/m ²
0	8.4812073*exp(0)	8.4812
0.002	8.4812073*exp(-0.5873*0.002)	8.47125
0.004	8.4812073*exp(-0.5873*0.004)	8.4613
0.006	8.4812073*exp(-0.5873*0.006)	8.45138
0.008	8.4812073*exp(-0.5873*0.008)	8.44145
0.01	8.4812073*exp(-0.5873*0.01)	8.43154
0.012	8.4812073*exp(-0.5873*0.012)	8.24164
0.014	8.4812073*exp(-0.5873*0.014)	8.41175
0.016	8.4812073*exp(-0.5873*0.016)	8.401884
0.018	8.4812073*exp(-0.5873*0.018)	8.39202
0.02	8.4812073*exp(-0.5873*0.02)	8.382168

F. Evaluation of the solution current density (i_s)

$$i_s = uzFC_f (e^{mx} - 1) \quad \dots(3.25)$$

$$i_s = 0.066314 * 96487 * 2 * 1 (e^{-0.5873x} - 1)$$

$$i_s = 12796.99(e^{-0.5873x} - 1) \text{ and multiplying the results by } -1$$

to get positive values of current

x(m)	i_s	Value in A/m ²
0	12796.99*(exp(0)-1)	0
0.002	12796.99*[exp(-0.5873*0.002)-1]	15.0225
0.004	12796.99*[exp(-0.5873*0.004)-1]	30.027
0.006	12796.99*[exp(-0.5873*0.006)-1]	45.0146
0.008	12796.99*[exp(-0.5873*0.008)-1]	59.984
0.01	12796.99*[exp(-0.5873*0.01)-1]	73.1797
0.012	12796.99*[exp(-0.5873*0.012)-1]	89.871
0.014	12796.99*[exp(-0.5873*0.014)-1]	104.778
0.016	12796.99*[exp(-0.5873*0.016)-1]	119.6875

0.018	$12796.99 * [\exp(-0.5873 * 0.018) - 1]$	134.5695
0.02	$12796.99 * [\exp(-0.5873 * 0.02) - 1]$	149.43

الخلاصه

لقد تم في هذه الدراسة انجاز نمذجه لمفاعل كهروكيمياوي يعمل تحت تأثير التيار المحدد. وكانت الظروف التي اجريت عليها النمذجه هي :- انتظام الزمن , الجريان خلال الحشوه احادي البعد. وان التفاعل الذي تمت دراسته هو ترسيب ايونات النحاس الموجوده في محلول الكتروليتي يحوي كبريتات النحاس وحامض الكبريتيك كمحلول مساند بفرض غياب التفاعل العرضي ونوع الحشوه هو حبيبات كروي الشكل. تمت دراسته تأثير كل من المتغيرات الاتيه على كل من :- توزيع التركيز, توزيع الجهد , سرعه التفاعل وكثافه التيار في المحلول الالكتروليتي وهذه المتغيرات هي (معدل الجريان للمحلول, تركيز المحلول الالكتروليتي الابتدائي وسمك الحشوه).

ان طبيعه سلوك المفاعل تم الحصول عليها من خلال حل معادلات موازنه الكتله وموازنه الجهد أنيا حلا تحليليا.

وقد وجد ان معدل الترسيب يزداد في الحالات الاتيه:-

1. زياده معدل جريان المحلول بسبب ان الطبقة المتاخمه للانتشار قرب سطح القطب السالب تصبح اقل سمكا .

2. نقصان سمك الحشوه .

3. زياده تركيز المحلول الالكتروليتي بسبب زياده معدل الانتقال قرب سطح القطب السالب .

لقد تم اجراء مقارنه بين نتائج النمذجه الحاليه لتوزيع الجهد مع النتائج العمليه لبحث

Lacoste و Olive ولوحظ ان المقارنه ناجحه من حيث تقارب النتائج.

دراسة مفاعل كهروكيمياوي يعمل تحت تأثير انتقال الكتله لازاله
ايونات المعادن

رساله

مقدمه الى كليه الهندسه جامعه نهرين
وهي جزء من متطلبات نيل درجه ماجستير علوم
في الهندسه الكيمياويه

من قبل

أسن قصي ناجي

بكلوريوس علوم في الهندسه الكيمياويه 2004

1428
2008

ذو الحجة
كانون الثاني